THE EFFECT OF TEMPERATURE AND CONFINING PRESSURE ON FLUID FLOW PROPERTIES OF CONSOLIDATED ROCKS

by

Francis J. Casse

November 1974

This report was prepared originally as a dissertation submitted to the Department of Petroleum Engineering and the Committee on the Graduate Division of Stanford University in partial fulfillment of the requirements for the degree of Doctor of Philosophy.

ACKNOWLEDGEMENTS

I welcome this opportunity to thank my advisor, Dr. Henry J. Ramey Jr., for the guidance and suggestions he provided throughout my research work.

I am also indebted to Dr. Sullivan S. Marsden who helped me through several tight spots in this work.

I also want to express my sincere appreciation to Norio Arihara, a graduate student of the Department for his friendly help and encouragement.

Peter Gordon, The School of Earth Sciences machinist deserves credit for several modifications made to the original equipment.

The financial support provided by Tenneco Oil Company and Mobil Oil Company, which made this work possible, is gratefully acknowledged.

Finally, I wish to express my gratitude to my wife Jackie, who typed this dissertation and gave me constant encouragement, and to my son Nicolas who managed to bring joy at the most difficult times in cy research. I dedicate this work to both of them.

ABSTRACT

Recent work on the effect of temperature on relative permeability suggested that absolute permeability was also a temperature dependent property of rocks.

Equipment originally designed to perform dynamic displacements through consolidated sandstone samples was modified and used to measure absolute permeability under conditions of elevated temperature and overburden pressure. Several fluids were used to make these measurements, namely, distilled water, white mineral oil, nitrogen and helium.

In light of the unique results obtained with distilled water, i.e., significant permeability reduction at high temperature, changes in flow properties due to rock-fluid interaction were given particular attention. Whenever a temperature dependence was evidenced, the combined effect of pure mechanical stresses and thermally induced stresses was studied, and an additive effect was generally observed.

Finally, during the course of the gas flow experiments, the effect of temperature on gas slippage and turbulence coefficient was also analyzed, and close agreement between experimental results and theory was found.

TABLE OF CONTENTS

LIST OF TABLES

LIST OF ILLUSTRATIONS

LIST OF ILLUSTRATIONS (continued)

LIST OF ILLUSTRATIONS (Continued)

I. INTRODUCTION

Several workers in the last decade have found relative permeability to be a temperature-dependent property of rocks. However, the lack of consistency in the results that they obtained, and the need for more conclusive data motivated further investigation in this area. With this objective in mind, additional experimental research was conducted in the late 1960's by Weinbrandt [1]. His findings suggested that not only relative permeability but also absolute permeability of fired consolidated rocks could be a function of the temperature level. Firing at 940°F was done to oxidize any organic matter in the core and possibly to deactivate the clays.

The validity of this speculation was checked in 1972 by the present author [2] by measuring absolute permeability to water at conditions of elevated temperature for two types of fired sandstones. The experimental apparatus used was the same as for the relative permeability measurements, and temperature was found to have a strong effect upon absolute permeability.

In all reservoir engineering calculations, absolute permeability is a basic parameter and it has been traditionally

measured at room conditions, with the implicity assumption that it changes only with loading pressure, not with temperature, Therefore, immediate interest was generated by the above mentioned preliminary results, and the obvious need for additional information motivated the present study,

The preliminary study had been conducted with distilled water only as a saturating fluid, and little attention had been given to the possible influence of such phenomena as clay swelling or molecular interaction at the surface of the rock because the cores had presumably been deactivated by firing. In order to provide a clue as to what actually caused the permeability to decrease with increasing temperature, it was decided to use other fluids such as inert gases and a mineral oil, and to look for possible fluid entrapment at high temperature.

The speculation was also made that thermally induced mechanical stresses were responsibl-e for the changes observed in fluid flow properties, Stresses of the same nature can be induced by purely mechanical action, such as increasing the confining load of the rock samples studied. The changes in fluid flow properties that have been reported due to these mechanical stresses are somewhat analogous to the changes observed with temperature. Therefore, it was also decided to vary the overburden pressure and to study simultaneously the effect of temperature and pressure on the fluid flow properties of various sandstones.

Finally, one more objective of the study was to use the gas flow data to determine values for the Klinkenberg slip factor and the turbulence factor at elevated temperatures.

II. SURVEY OF LITERATURE

After giving a formal definition of the permeability of a porous medium, Muskat[3] makes the following comment: "It is thus a constant determined only by the structure of the medium in question and is entirely independent of the nature of the fluid". Since the structure of a porous medium can be altered by subjecting this medium to a high temperature change, it is interesting to note that the above comment does not exclude the possibility of a temperature dependence for permeability. Yet, even though the statement has never been explicitely made that permeability is independent of temperature, it has been common practice in reservoir engineering calculations to use a single value of absolute permeability throughout a range of temperatures. This tendency to believe that permeability would not be affected by temperature, at least in the hydrology literature, is perhaps due to an evolution in terminology that led to the present definition of absolute permeability. The proportionality factor that relates the velocity of a fluid to the pressure gradient in Darcy's law, is now termed the mobility of the fluid. For single phase flow it is the ratio of the absolute (or intrinsic) permeability to the fluid viscosity, i.e., $\frac{k}{\mu}$. It is not uncommon, however, that this ratio itself be termed the "permeability" in the hydrology literature; in many papers one may read that "permeability is inversely proportional to the fluid viscosity", and that

"the influence of temperature on permeability must be considered through changes in the fluid properties".[4] It is possibly this misconception even after permeability and viscosity were clearly separated, that prevented basic research in this area earlier.

It is only in the late 1960's that changes in absolute permeability were observed with temperature. In 1968, Greenberg, et al.,[5] reported data on the permeabilities to water of nine artificially-consolidated hydrological porous medium samples, for a limited temperature span (80-140°F). The general trend showed either slight to moderate decreases in permeability or else no change at all with increasing temperature, with the exception of increases in two cases. The changes observed were attributed to microstructural rearrangements in the matrix geometry of the samples which had a rough and irregular surface texture, whereas samples with relatively smooth surfaces showed no apparent permeability changes. It must be noted that all the core samples tested were artificially consolidated with phenolic resin or by sintering, and that no confining pressure was applied around the cores.

In 1969, Afinogenov[6] reported a considerable reduction of permeability with increased temperature (up to 100-fold between -3°F and 200°F). The validity of these results, however, is questionable, because his data were obtained by a continuous method which probably did not allow for isothermal conditions to be reached. Tenperature increased from 70°F to 200°F in ten minutes only, and all of the data were obtained curing that brief time interval. No mention was

made about possible clay content of the samples. Confining pressures from 300 psi to 15,000 psi were used, but no attempt was made to study the combined effect of temperature and confining pressure on absolute permeability. Instead a separate investigation of the effect of hydrostatic pressure on permeability at room temperature was conducted. Again extreme reduction of permeability was observed at high confining pressures. Qualitatively, these results agreed with previously published work[7 to 12], but quantitatively the decrease observed was much greater than one might intuitively expect.

The effect of radial and/or axial stress on the physical properties of rocks has been studied by several investigators. A review of earlier work was made in 1967 by Wilhelmi and Somerton[7]. They measured simultaneously pore and elastic properties of rocks under a wide range of triaxial stress conditions. One of the first contributions in that area had been made in 1972 by Fatt and Davis[8]. They showed that permeability at 15,000 psi confining pressure could be 25 to 60% smaller than permeability at zero confining pressure, depending on the type of rocks studied, Generally speaking, the higher the permeability, the higher the percentage of reduction, although the opposite trend was observed by McLatchie, et al.,[9] The discrepancy was attributed to the fact that in the former case clean sandstones and limestones had been used, whereas in the latter case the cores used had a high clay content.

In 1963, work on the effect of overburden pressure on permeability was extended by Gray, et al.[10] to sandstone permeability anisotropy. Permeability reduction was shown to

be a function of the ratio of radial to axial stress, with maximum reduction evidenced under uniform stress, i.e., when the axial stress is equal to the radial stress. As will be seen later, the present work was accdmplished under conditions of uniform stress,

Further refinement in this area was obtained by considering the effect on permeability of the net confining pressure, defined as (confining pressure - α xpore pressure). Several investigators have found that a good value for α is 0.85. Among them, Dobrynin[11] made the assumption and effectively observed, that the changes in several physical properties of rocks under pressure, including permeability ana porosity, are controlled to a large extent by the pore compressibility of these rocks. This important observation may provide a clue to the discrepancy between the results presented by Fatt[8] and McLatchie[9]. The contribution of highly compressible material to permeability reduction was pointed out by Zoback[12], in an attempt to develop a conceptual model of Berea sandstone. His model consisted of a relatively incomnressible quartz framework surrounding a highly compressible matrix material and a single cylindrical capillary. His simplified theory was supported by experimental results showing that high pore pressure can affect permeability to an even greater extent than toes the confining pressure,

Several investigators simultaneously studied the effect of overburden pressure on several rock properties [7,11,13]. One of these properties is porosity, which evidently has an

important bearing on permeability. Porosity has been acknowledged to change with overburden pressure in the same direction as permeability. However, it has proven impossible to correlate the changes in porosity with the changes in permeability. A large permeability variation may be the result of a significant change in porosity for certain types of rocks, whereas the same permeability variation may occur with practically no porosity change for other types of rocks,

Nevertheless, intuition and all experimental results indicate that a decrease in porosity is always accompanied by a reduction in permeability. It would be therefore of considerable interest for the present study to know how porosity may be expected to vary with temperature, Unfortunately information in the literature is limited to speculations that porosity of rocks will decrease when temperature is increased. These speculations are generally substantiated by application of indirect studies of other temperature dependent rock properties, For instance, Sanyal, et al. [14] recently investigated the effect of temperature on electrical resistivity of porous media, As a result of their findings they speculated that both porosity and permeability should decrease with temperature increase, but that porosity changes were too small to explain the changes observed in the other rock properties. In later work on the effect of temperature on capillary pressure properties of rocks, the same authors (15) were able to draw similar conclusions, yet as the result of a different line of reasoning,

An attempt to derive an analytical expression for the change6

of porosity with temperature appeared in Okandan's work (16). Her simplified theoretical approach indicated that a porosity reduction should be expected when temperature is increased, but also that the magnitude of the reduction would be much too small to be detected by means of any conventional method, The important point, however, on which there is general consensus is that temperature will cause porosity to be reduced to some extent. The implications for the present work are well expressed by the following quotation from Muskat (3): "It is evident that any alteration of a given material which produces a decrease in porosity must necessarily result in a decreased permeability, For the reduction in porosity of a given material implies a decrease in size of the pores and hence an even greater percentage change in permeability". This, of course, is particularly true for the range of temperatures of interest in this work, i.e., 75°F - 350°F.

At temperatures well above 500°F consideration must be given to other phenomena such as decomposition of rock minerals, and permanent structural damage due to thermal stresses, Somerton (17) et al. reported that at room temperature, such damage may result in permeability increases of up to 50% for cores that had been subjected to 1500°F under a confining pressure of 1500 psi. Permeability was measured at room temperature using a standard air permeameter, before and after heating the samples. No permeability changes were reported in the range 75-350°F. This last result in itself is very interesting, Although it doesn't show how permeability varied

between 75°F and 350°F, it indicates that no hysteresis was observed after the samples were allowed to cool to room tenperaturc.

All the above mentioned observations show that structural deformations, whether due to mechanical or thermal stresses, do affect pore properties of rocks. Because of the analogy between these two types of deformations, it seemed appropriate in the present work to study their effects simultaneously and hopefully to show that there is a strong interdependence between temperature and confining pressure. The importance of this interdependence had riot been recognized initially, mainly because changes in flow properties with temperature were first thought to be the result of a change in fluid properties rather than rock properties. Accordingly, the work that has been aonc since the early 1960's on the effect of temperature on relative permeability [18-22] did not consider confining pressure an important parameter. Similarly, the preliminary stages of the present work were obtained at a constant overburcien pressure of 2,000 psi [22] ana temperature had been isolated as the only parameter affecting relative and absolute permeability,

To summarize the foregoing review, rcccnt findings suggest that research on the effect of temperature on rock permeability must be conducted, mainly because of the lack of information in this area. Deformation of rocks and permeability changes due to purely mechanical stresses have been thoroughly

investigated and an analogy between thermal and mechanical stresses may be anticipated. Therefore, a study of flow properties of rocks under a combination of thermal and mechanical stresses seems necessary.

III. EXPERIMENTAL EQUIPMENT

The original equipment was designed for water-oil relative permeability measurements and was described in detail by Weinbrandt (1). The main components, namely, the oven, the core holder, and the pressure measuring and recording devices, remained unchanged. But absolute permeability runs do not require dynamic displacements and consequently, several modifications were made to the fluid flow controlling devices.

1. GENERAL DESCRIPTION

Dynamic displacements were characterized by rapid response to change and continuous recording of transient flow parameters, They were also of sufficiently short duration so that the temperature staged. constant throughout the runs. On the other hand, absolute permeability runs require steady state and long-term, isothermal conditions. Therefore, emphasis was placed on maintenance of constant running conditions over a relatively long time. The constant rate, positive displacement pump was eliminated for it only had a 4-minute maximum running time before recharging. Instead, liquid flow vias controlled by microregulating pumps with unlimited running time, Gas flow was supplied from high pressure cylinders and delivered through finely adjustable pressure regulators.

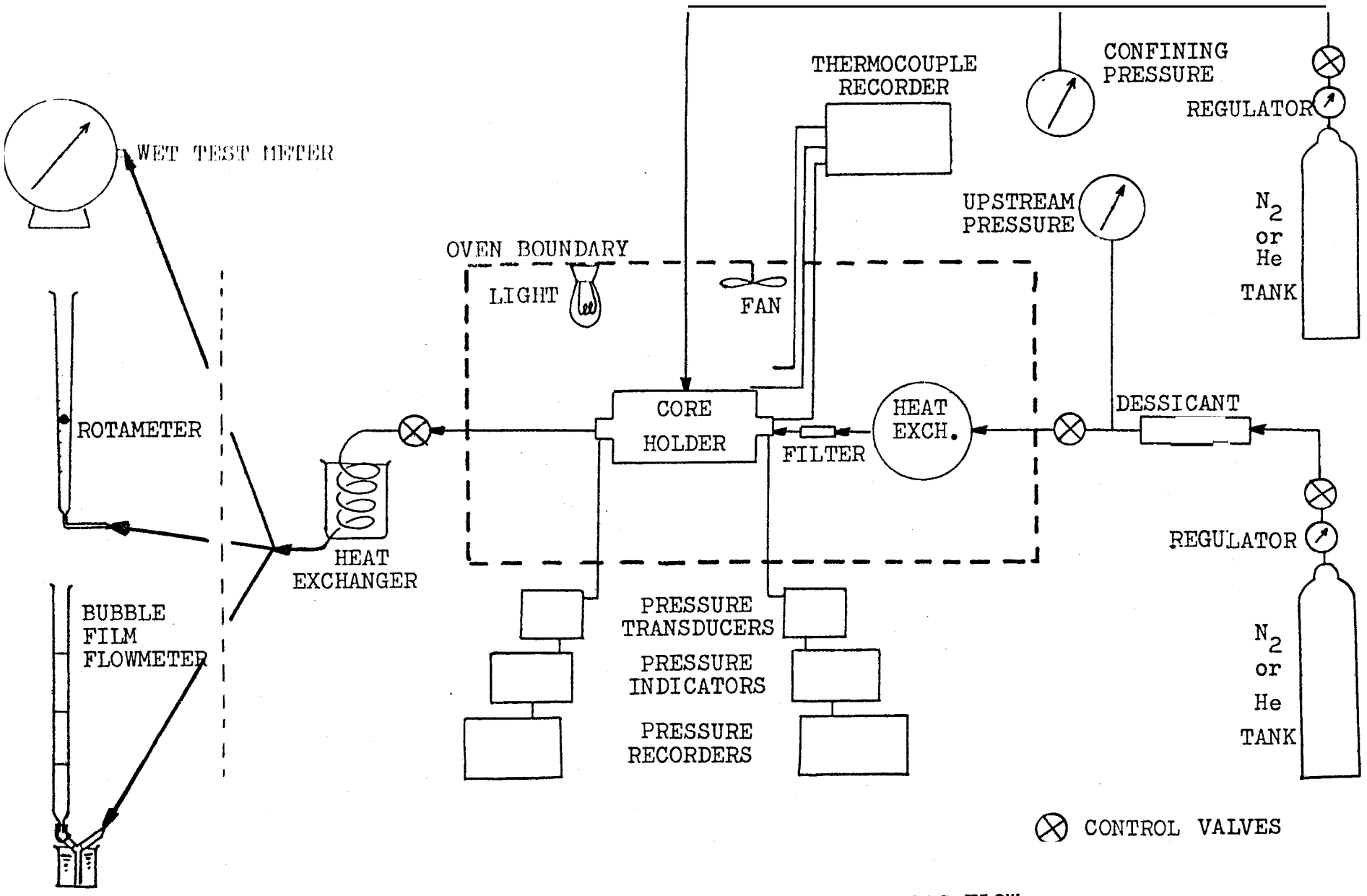

FIGURE 1 - SCHEMATIC DIAGRAM OF APPARATUS - GAS FLOW

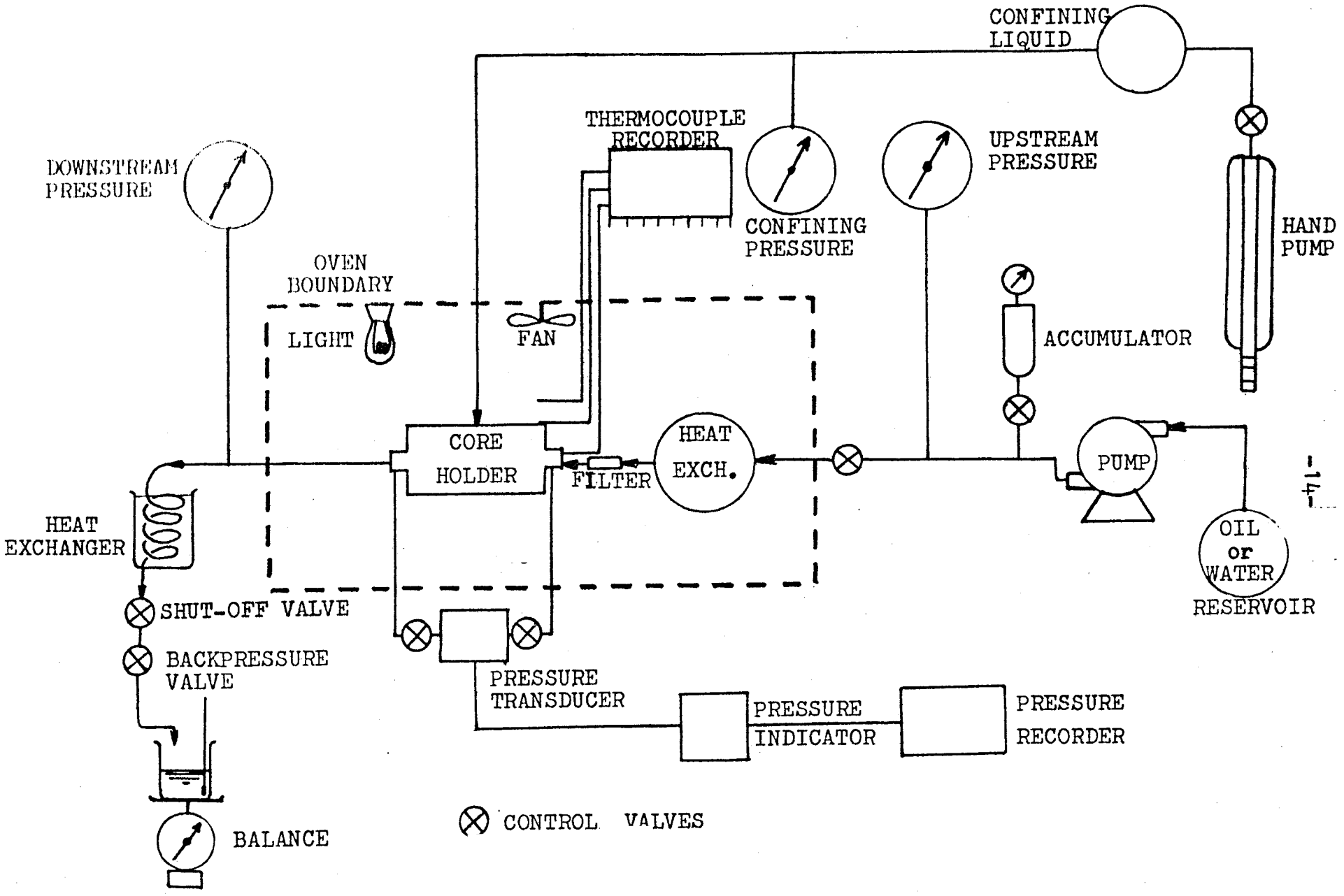

FIGURE 2 - SCHEMATIC DIAGRAM OF APPARATUS - LIQUID FLOW

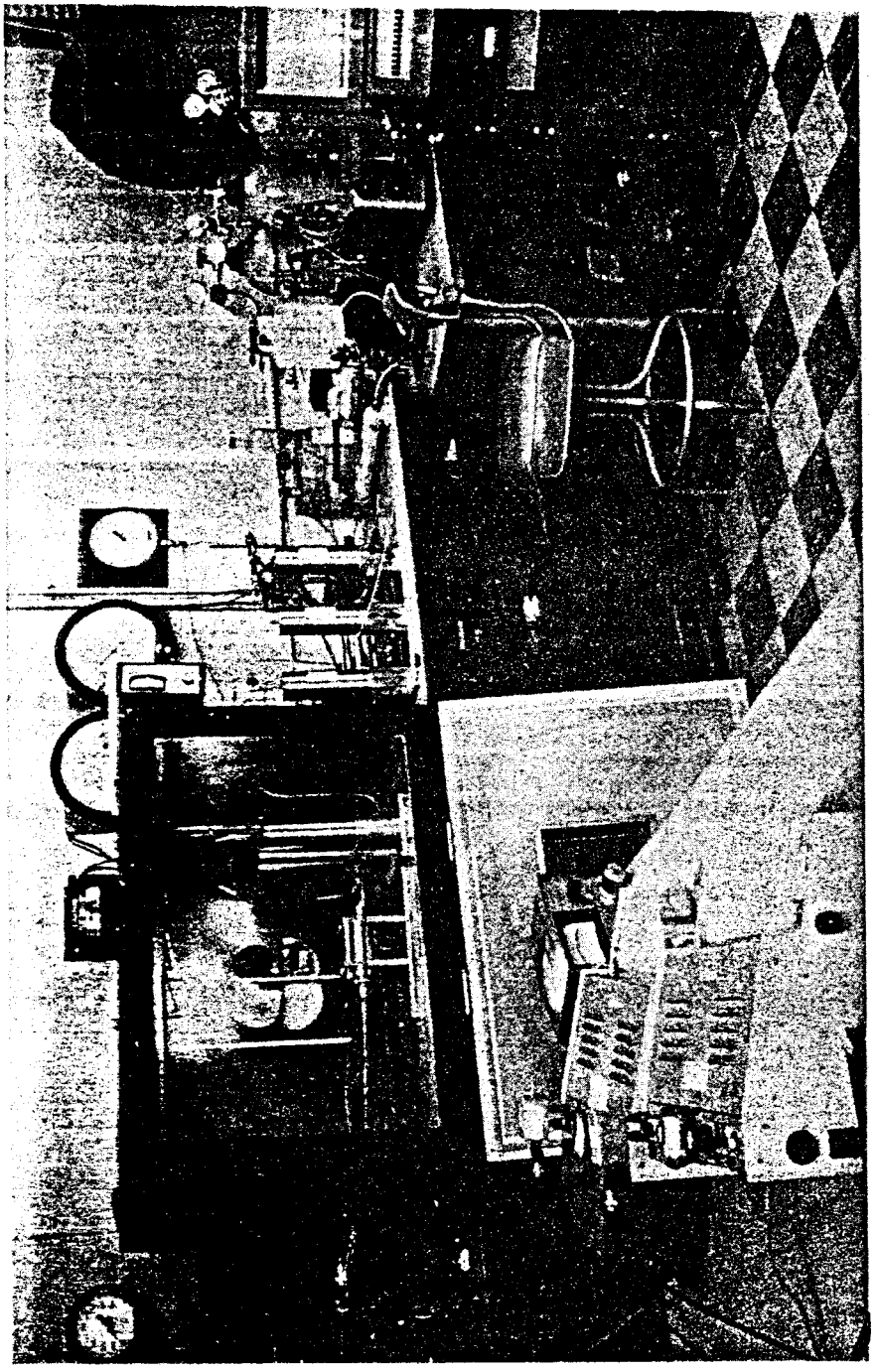

FIGURE 3 - PHOTOGRAPH OF EQUIPMENT

In order to measure the core and fluid temperature, a thermocouple was placed at the inlet face of the core, and temperature was recorded continuously during the runs. The core holder assembly was placed in an air bath that maintained run temperature. Material used in the cell, reservoirs, tubing and fittings was 316 stainless steel, which has excellent corrosion resistance.

A schematic diagram of the equipment is presented in Figs. 1 and 2. The former shows the arrangement for gas flow, while the latter is for liquid flow. A photograph of the equipment is shown in Fig. 3.

2. CORE HOLDER

The core holder is a Hassler rubber sleeve type. (see Fig. 4). The rock specimen to be studied is held in a "Viton A" rubber sleeve, between an upstream plug which is inmobile, and a downstream plug which moves horizontally and adjusts to the core length. The upstream plug has a pressure tap A, two taps for inlet flow B, and a thermocouple well C. Either liquid or gas pressure can be applied around the sleeve.

Since the downstream plug is mobile, one can see that both axial and radial confining loaas are simultaneously applied t the core.

It was observed that Viton sleeves, even $\frac{1}{8}$" thick, are slightly permeable to gases. Such a "leakage" is too small

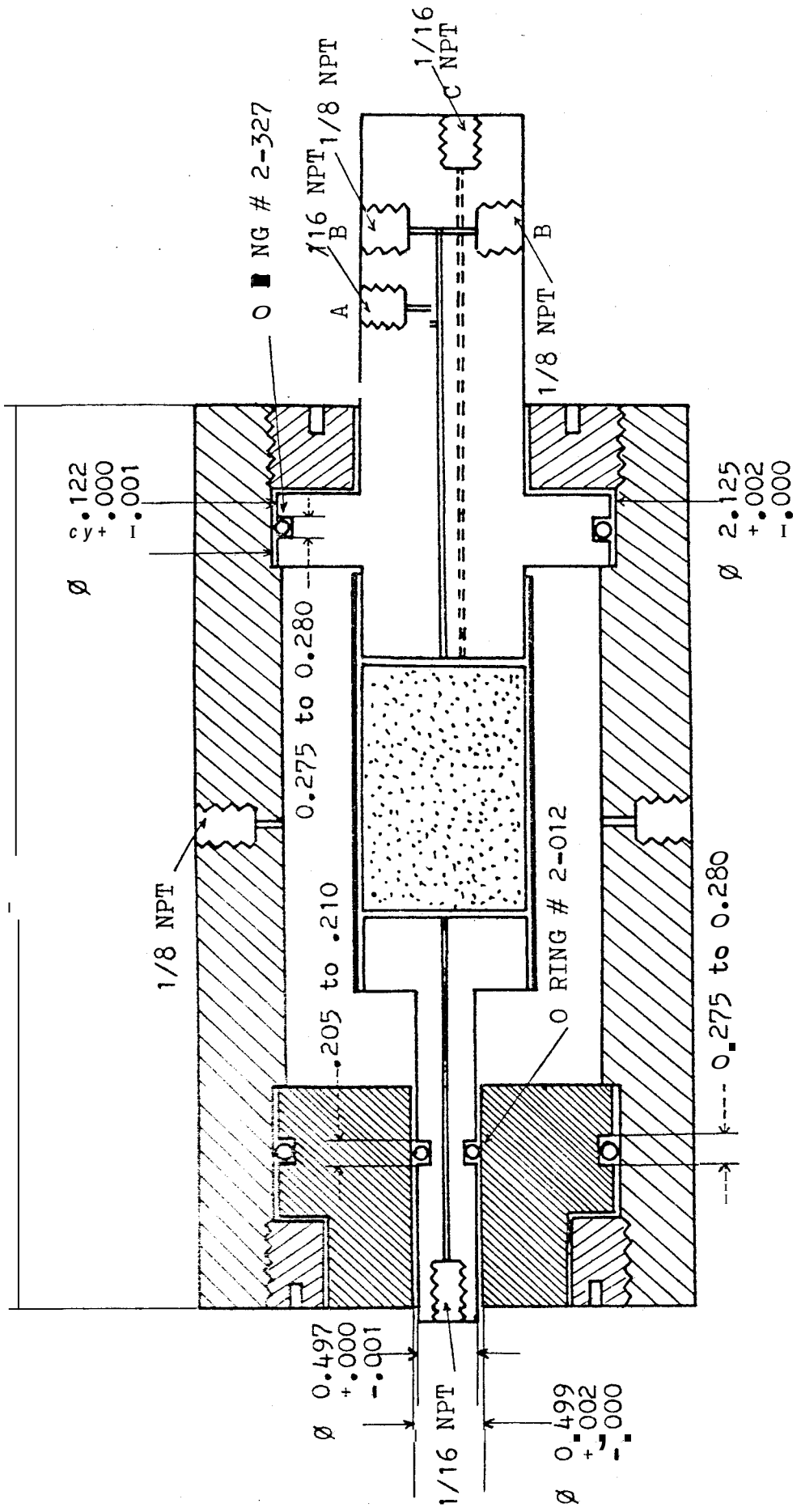

FIGURE 4 - CORE HOLDER

to affect gas flow, but would possibly create a residual gas saturation when liquid is flowing through the core. Therefore, it seemed appropriate that the confining fluid used around the sleeve be the same as the saturating fluid within the core. At the came time, this precaution prevented possible contamination of the core in the event that some of the confining fluid would seep into the core at either end of the sleeve over a long period of time.

3. OVEN AND TEMPERATURE CONTROL

The core holder assembly is placed in a 24 cubic foot oven. Four kilowatts of power are applied to the heating elements by an API model 4010 power pack and an API model 228 temperature controller. The thermocouple that triggers the output pulses of the controller can be placed at any location inside the oven. Since the objective is to bring the core to the desired temperature, the most efficient heating cycle has been found to result when the thermocouple sensor is tightly fastened to the core holder. A fan provides adequate air circulation and the oven is equipped with a light and a window.

Temperature is monitored by a 12 channel thermocouple recorder with iron-constantan thermocouples.

One thermocouple measures the temperature of the core itself, as vias pointed out in the previous section. The others are placed at different locations in the oven. It

was found that control temperature is reached in the air bath within $\mp 0.5^{o}F$ after about an hour, but approximately another half hour is needed for the core to reach the test temperature.

4. PRESSURE RECORDING DEVICES

Pressure drop across the core for liquid flow was measured with a Pace model KP15 differential pressure transducer and a Pace model CD25 transducer indicator. The range of pressure drops was handled by use of the proper diaphragm in the transducer (1 psi, 5 psi, 25 100 psi or 500 psi maximum differential pressure), These transducers offer an accuracy of 1% of the reading. A Heath Kit model EU-208 electronic recorder was connected to the inaicator and provided a permanent record of the pressure, All three instruments were calibrated using a Barnett Dead Weight Tester. Overall accuracy of the pressure measurement was 0.3% of the total scale,

For gas flow *an* additional set of the three instruments was added to the equipment.

5. FLOW RATE MEASURING DEVICES

A. GAS FLOW

Depending upon the value of flow rate Q, gas flow measurements were made using a stop watch and one of the following three instruments:

- a Wet Test Meter for high flow rates, i.e.:

  $0.5\ ft^3/hr < q < 20\ ft^3/hr$

- a Rotameter for intermediate flow rates, i.e.:
  $0.01\ ft^3/hr < q < 1\ ft^3/hr$
- a Burette (Bubble film method) for small flow rates, i.e.:
  $0.001\ ft^3/hr < q < 1\ ft^3/hr$

This last instrument proved to be the most accurate and the most reliable, because of its simplicity. The vertical part of a Y-shaped tube is plunged up to the throat in a soap sol-ution (See Fig.1). The gas flow to be metered enters through one of the branches and bubbles into the other branch and then up into the vertical burette, until the pressure required to push the bubbles becomes sufficient to push the soap solution down the vertical part of the Y-tube, thus leaving the throat open to flow. Then the flow rate is obtained by simply measuring the time it takes for a bubble to traverse a known volume in the burette. Because the pressure required to displace tho bubbles was always less than 0.01 psi, this method essentially provided flow rate determinations at room conditions.

The bubble film method is highly accurate and repeatable. It was used to calibrate the rotameters, at least in the low values of their working ranges. The rotameters consisted. of a laboratory kit of variable area flowmeters employing "Tri-Flat" tapered tubes. Proper combination of the set of tubes and floats available with the kit makes it possible in theory to measure flow rates of gases ranging from 0.01 to 60 ft^5/hr.

But practically, because these flowmeters are very sensitive to room conditions and require both temperature and pressure corrections, the use of the bubble film method or the Wet Test Meter vias preferred, whenever possible.

B. LIQUID FLOW

Although the rotameters used for gas flow cou d aiso be calibrated for liquid flow, oith the advantage of giving instantaneous values of the flow rate, a very accurate mass flow rate determination was preferred. At steady state, the mass flow rate is constant throughout the system and cans thus be measured. at any point along the flow line. This was accomplished by weighing small volumes of the effluent liquid on an analytical balance over a known period of time, The sensitivity of the balance is ± 0.1 s. (Therefore for a tine interval of more than 100 seconds, the mass rate can be *de*termine? with less than 0.1% error).

6. PUMPS

In order to reach steady state, flow must be maintained over a period of time sufficient that all variables, e.g., pressures, temperature and flow rate, remain constant, Constant pressure can only be obtained if no pulsation is generated by the pump. A positive displacement pump consisting of a piston driven into a cylinder by a synchronous motor would serve that purpose, and immediately deliver constant rate. These features had justified the use of such a pump for dynamic

displacements (1). On the other hand, its limited running time range (4 minutes at 25 cc/sec) would make it impractical for steady state runs and repeated measurements. A more convenient way of handling this problem consisted. in using the two micro-regulating pumps that were used before to re-charge the positive displacement pump. The water pump is a Lapp "Microflo" Pulsafeeder with a dial indicator calibrated in 1000 increments.

The oil pump is a Whitey Micro-regulating Laboratory Feed pump with a dial indicator also calibrated in 1000 increments, Both pumps create large pressure pulsations when delivering at high pressures. In order to eliminate pulsations, accu-mulators were inserted along the flow lines and proved to be effective in almost totally damping the pulsations, Constant pressures were maintained at both ends of the core,

The positive displacement pump vias only used occasionally to double check the results obtained with the other pumps.

7. HAND PUMP

An Enerpac hydraulic hand pump provided easy adjustments of the confining pressure from 0 to 10,000 psi. Chevron white mineral oil No.15 was the liquid compressed by the pump, so that the pump could be connected airectly to the core holder for oil permeability measurements. For water permeability measurements, a water reservoir was inserted between the pump ana the core holder, in order to match confining and flowing liquid. Incremental changes in confining pressure were obtained

by use of two consecutive valves and/or the hand pump,

8. BACKPRESSURE VALVE

Gas pressure was held on the efflux liquici in a large collector vessel in the early stages of this work. But for most of this study, backpressure was regulated by means of a fine metering needle valve, This valve served several purposes. The main purpose was to keep water from boiling at temperatures above 212°F. Another use was to simply change the pore pressure level, in order to obtain any desired value of the net confining pressure. A third use was to change the flow rate, and hence the pressure drop across the core, in order to get a multipoint determination of permeability. Finally, keeping the downstream pressure at a sufficiently high level prevented gas evolution from the liquid, thus guaranteeing that the core remained 100%liquid filled.

9. HEAT EXCHANGERS

It is essential that temperature remains constant during a run. Because the fluids enter the oven at room temperature, a large size reservoir was installed inside the oven before the core holder. Cold fluid entered at the bottom of the reservoir, while hot fluid left from the top. Because of the large size of the reservoir and the small flov rates that viere

used with liquid flow, the temperature of the liquids leaving the reservoir and entering the core vias found to remain constant and to be equal to the desired test temperature during the entire run. When gas was flowing, much higher rater were attained, especially when turbulent flow was induced. A tendency for the temperature to drop was observed, in spite of the low heat capacity of the gases, This effect was eliminated by filling the reservoir with steel wool, thus improving the heat exchange, At the other end of the system, fluids must be cooled prior to flos rate determination, This was accomplished by letting the fluids flow through a coil immersed in a constant temperature water bath.

10. GAS SOURCES

Gas flow through the samples was supplied from high pressure cylinders, and regulated by a two-stage adjustable regulator equipped with a relief valve. Initial cylinder pressure was 2500 psi and delivery pressures ranged from 5 psi to a maximum of 450 psi.

Small pressure increments were made possible by use of a rotating knob which had eight revolutions for the whole pressure range. Confining pressure for gas flow experiments was also supplied ?=~a high pressure cylinder and regulated by a high pressure regulator capable of delivering up to 2000 psi,

IV. PROCEDURE

1. CORE PREPARATION

Three types of sandstones were used in this work, namely, Boise, Berea and Bandera sandstones, In order to provide a reproducible reference, core preparation prior to any run followed a well-defined program.

A diamond drill was used to cut one inch diameter cylindrical cores using tap water as the drilling fluid. These cores were then trimmed on a lathe with a carbide cutting tool to an approximate length of 2 inches, to insure that they were right circular cylinders. After trimming, the samples were extracted for 5 to 8 hours in a Dean-Stark type extraction apparatus at atmospheric pressure, The apparatus conforms to the Bureau of Mines Report of Investigations No.4004. Following extraction, the cores were ignited for at least 5 hours in a 500°C furnace. Tnis temperature was selected because it is high enough to oxidize organic matter, but lower than the decomposition temperature of calcium carbonate to calcium oxide. Then the cores were allowed to cool to room temperature over a period of at least 12 hours. Their length and diameter were recorded with 0.002 inch accuracy. Dry weight was measured with 0.0001 gm accuracy.

After ignition, the cores were saturated under vacuum with

the desired flowing liquid, i.e., either distilled, filtered, ueaerated water, or filtered, deaerated Chevron No. 15 white oil, Complete saturation was reached after the liquid-covered cores stayed for 2 or 3 hours under a vacuum of less than 1 inch Hg. Weight at 100%liquid saturation was recorded, in order to determine porosity by difference with the dry weight.

For nitrogen or helium flow, the air saturated cores were flushed with several pore volumes of the desired gas so that residual air was completely eliminated by diffusion,

2. REACHING RUN CONDITIONS

Permeability measurements began with placing the liquid- or air-saturated core in the core holder. For liquid. saturated cores, great care had to be exercised, so that no air would be forced into the core while it was pushed into the rubber sleeve, Whenever there was any doubt, the core and sleeve assembly was saturated again under vacuum until full saturation was restored.

Confining pressure was then applied, As mentioned earlier, the confining fluid was the same as the saturating fluid in order to avoid undesirable effects due to nossible leakage while pressurizing the system or after system was under pressure, A leakproof seal at both ends of the rubber sleeve was obtained by compressing the sleeve tightly with 20 gauge stainless steel wire aroun: the upstream and uownstream plugs,

The assembled system was then brought to the desired run temperature. As indicated in the aescription of the oven, this

step required about 1½ hours. While heating up, thermal expansion of the confining fluid would cause the overburden pressure to increase.

Repeated manual adjustments were therefore necessary to keep the overburden pressure within ten percent of its desired value, The effect on permeability of letting the pressure increase far beyond this range was also investigated in this work,

At that time, fluid flow was initiated and measurements of temperature, pressures and flow rate were made at regular time intervals. Steady state was assumed nhen no appreciable change could be detected in the above variables, and the corresponding values were then recorded.

3. GAS FLOW

Gas pressure was regulated upstream by a two-stage pressure regulator. Gas flow rate was regulated downstream by means of a needle valve. Pressures and flow rate were recorded at steady state. Detailed analysis of gas flow data is given in Appendix B.

A. GAS VISCOSITY

Nitrogen and Helium viscosities were calculated using Sutherland's formula : $\mu = \frac{A \times T^{1.5}}{B + T}$, where T is the temperature in ^{o}K. Values for A and B for Nitrogen and Helium were found in ref.35. For the temperature range considered in this work, the results yielded by the above

formula agree within less than 1% with publisher! experimental aata, These results are presented in Fig.8 and Table 4 in Appendix A,

B, FLOW RATE MEASUREMENT

The choice of the appropriate flowmeter was determined by the ranges of flowrates required by the type of flow under consideration, i.e., laminar flow or visco-inertial flow.

a, Laminar flow data

Laminar flow vias used to calculate the two basic parameters : extrapolated Klinkenberg permeability and Klinkenberg slip factor. Run conditions were characterized by small pressure drops across the core and a sufficient amount of back pressure. Accurate measurements were needed to determine the Klinkenberg straight line. Flow rates were measured with the bubble film type flowmeter at room conditions, as described in section III 4 A. Atmospheric pressure and room temperature were also recorded, and necessary corrections to flowing conditions were made.

b. Visco-inertial flow data

Visco-inertial flow provided data for calculation of the turbulence factor. Large flow rates were obtained by reducing the amount of backpressure and thus increasing the pressure drop across the core. Flowrate measurements were made using a Wet Test Meter or a calibrated set of Rotameters, The accuracy of these measurements was less than 5% in some cases,

which accounts for the scattering of the turbulent flow data. However, a great number of data points were obtained in the visco-inertial flow region, and a satisfactory analysis of the data was always possible,

C. PRESSURE MEASUREMENT

In the case of gas flow, the upstream pressure p_1 and the downstream pressure p_2 were both necessary for calculating permeability, rather than the pressure drop only. Therefore, two pressure transducers were used. For laminar flow, the values of p_1 and p_2 were close to one another. Maximum accuracy was obtained by measuring p_1 with one transducer and the pressure drop, Δp, with the other transducer. From these values, the mean pressure $p_m = p_1 - \frac{\Delta p}{2}$ was computed, and the difference $(p_1^2 - p_2^2)$ was calculated as

$$(p_1 + p_2)(p_1 - p_2) = 2\, p_m\, \Delta p, \text{ i.e.,}$$
$$p_1^2 - p_2^2 = \Delta p\, (2p_1 - \Delta p)$$

For turbulent flow data, when the pressure drop was no longer small compared to the mean pressure, separate measurement of p_1 and p_2 were taken.

4. LIQUID FLOW

A. LIQUID PREPARATION

Two liquids were used in this work, namely water and a mineral oil. Tap water was distilled in a Barnstead stainless

steel still. Following distillation, the water was filtered and deaerated under a vacuum of about 0.3 psia. A pH of 5.5 was measured, even after the distillation, filtration and deaeration, This low value of pH was attributed to high carbon dioxide content of tap water,

Data on water density and water viscosity versus temperature were found in the Steam Tables [37] and are presented in Fig.5 and 6.

Chevron White Mineral Oil No.15 was used for the oil flow experiments. It was filtered and deaerated in the same manner as described for water. White Mineral Oil No.15 is commercially available, and the physical properties of the oil may vary slightly from one batch to another, It was found that published data from Edmondson [18] and Davidson [19] differed by as much as thirteen percent at 300°F. Attempts to measure viscosity with a Brookfield Electro-Viscometer were unsuccessful, in that erroneously high values. of viscosity were measured at high temperature probably due to vaporization of light components of the oil.

A capillary tube viscometer was constructed in which viscosity could be measured under pressure, The procedure for these measurements is presented in detail in paragraph E, (below). The resulting oil viscosity data are shown in Fig.7. The oil density was determined by weighing a known volume of oil at several temperatures. It was found that oil density decreased linearly with increasing temperature, and the data. obtained were in excellent agreement with Davidson's [19] data. A

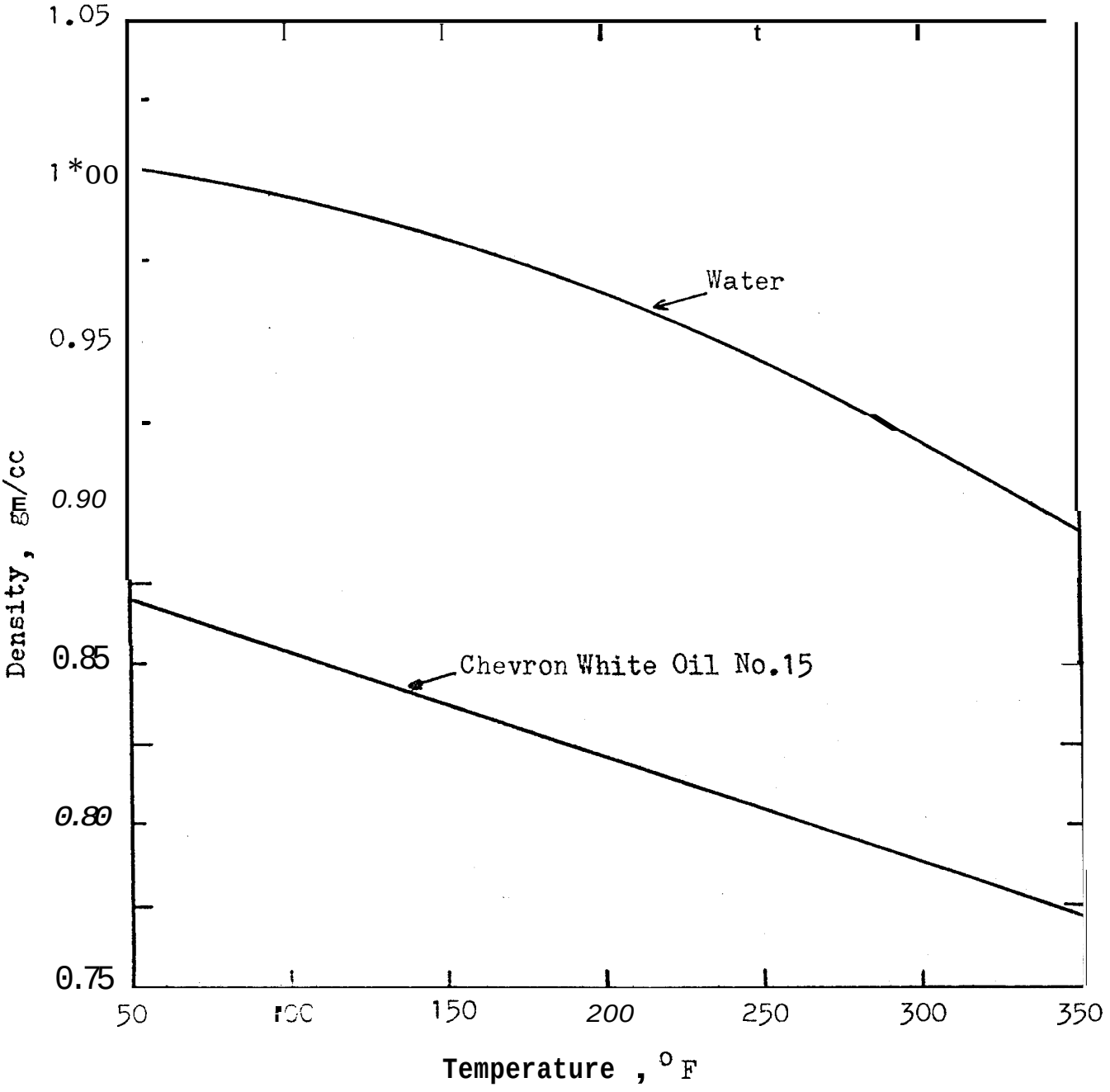

Figure 5. Densities of water and **Chevron White Oil** No.15 as Functions of Temperature.

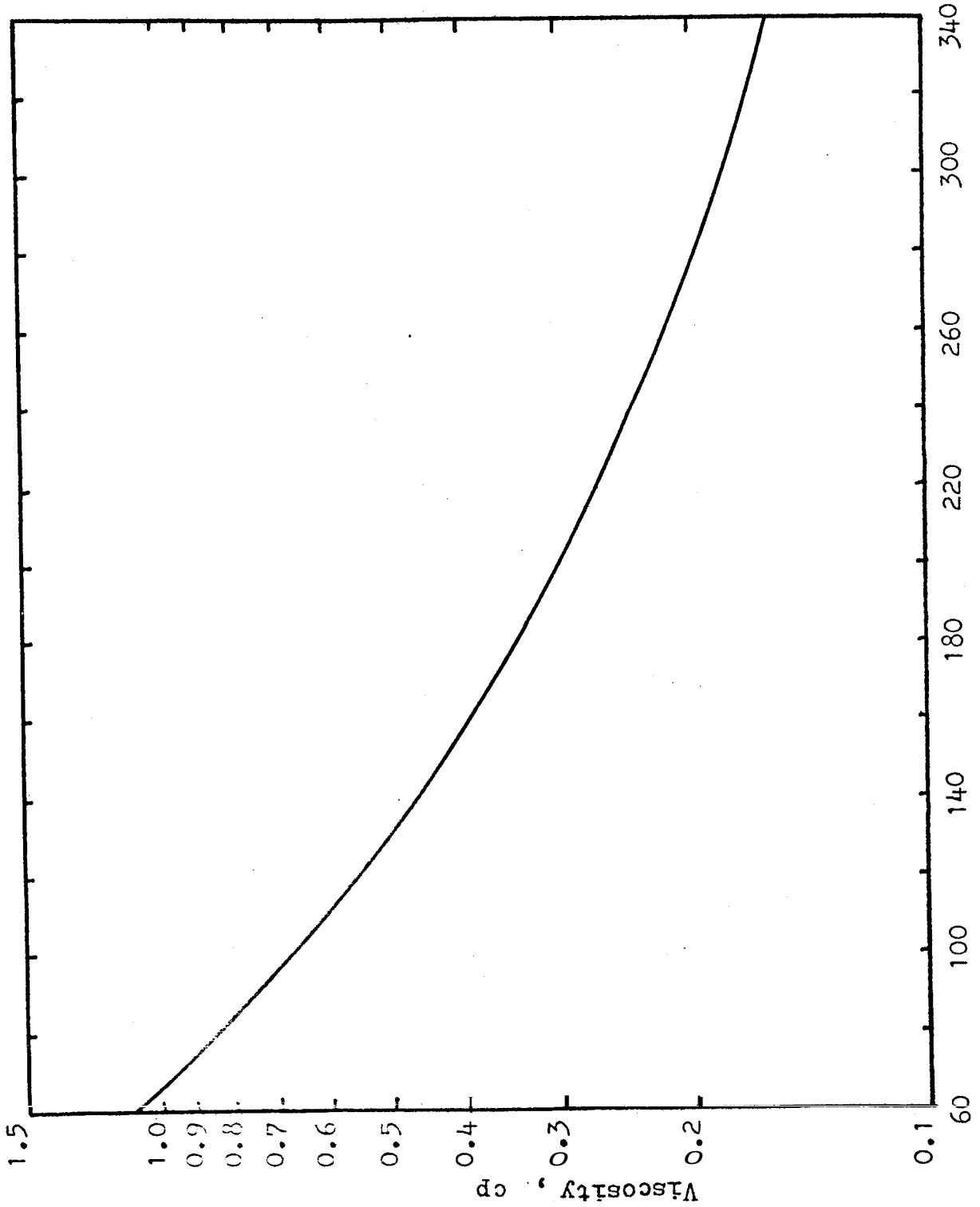

Figure 6. Water Viscosity as a Function of Temperature at 200 psig.

graph of oil density versus temperature is presented in Fig.5, and the data and results are listed in Table 3 in Appendix A,

B. BACKPRESSURE

Under atmospheric pressure, the boiling point of water is 212°F, and the initial boiling point of White Oil No.15 is 558°F. But evaporation of light components was observed at temperatures as low as 150°F at atmospheric pressure, Therefore, it was necessary to keep the liquids under a sufficient amount of pressure along the entire flow line, An exit flowing pressure of approximately 200 psi was held on the flow system by using the needle valve located at the downstream end of the flow system. Maintaining the flowing pressure at that level also had the effect of reducing the volume of air that might have been left in the pressure gauges, accumulators or transducer lines. The use of an accumulator in series with the pump made it possible to keep the flowing pressure from changing drastically, even when the flow was started or stopped.

C. FLOW RATE MEASUREMENT

Repeated measurement of the flow rate helped determine when steady state had been reachea. As mentioned earlier in the description of the equipment, the liquid effluent was weighed at room conditions over known time intervals, For high temperature runs, boiling of the liquid as well as evaporation were avoided by cooling the liquid in a coil immersed in a constant

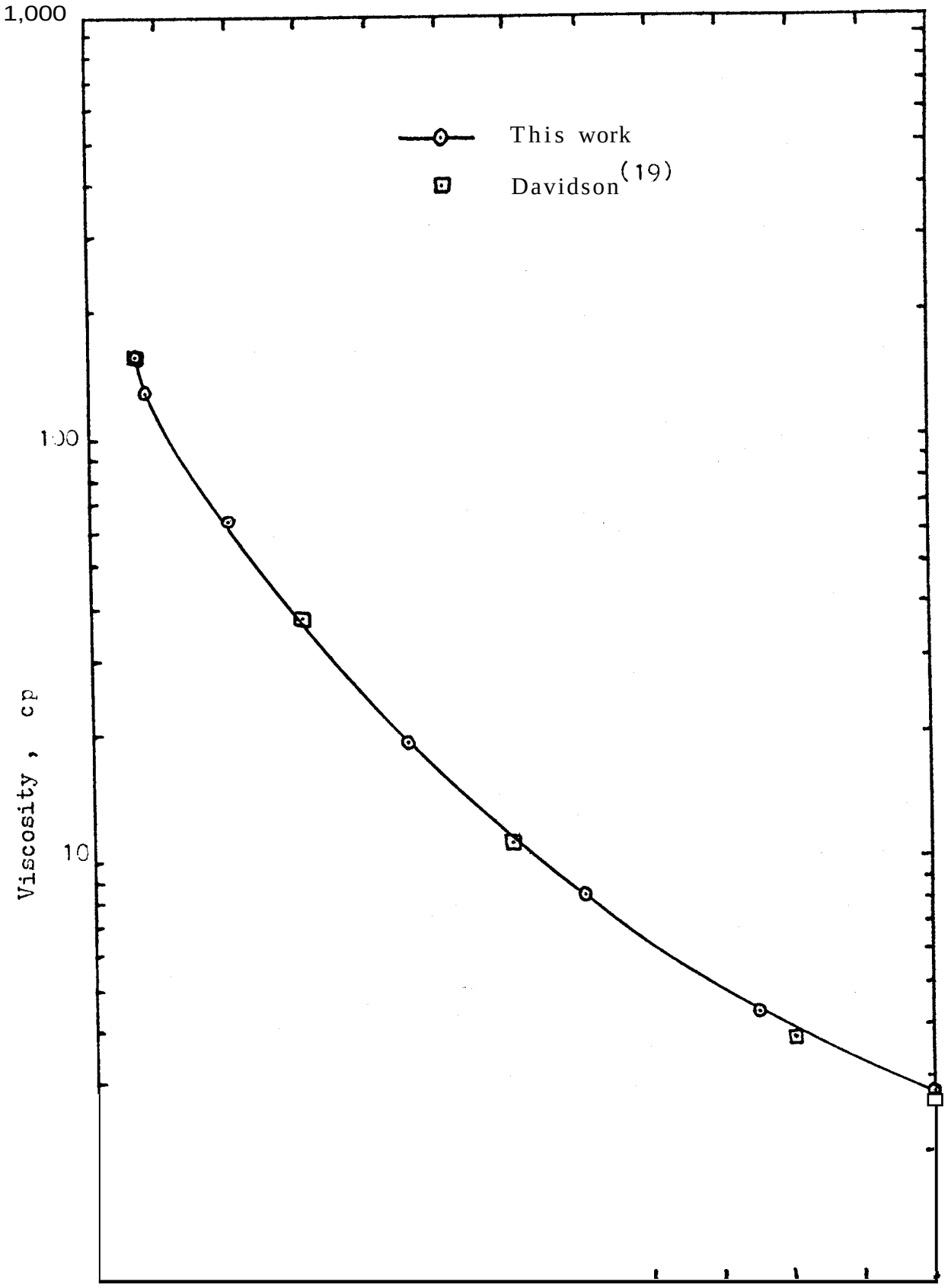

Figure 7 . Viscosity of Chevron White Oil No.15 Vs. Temperature at 200 psig.

temperature water bath, No correction to room conditions was necessary, because the mass flow rate at steady state was constant throughout the system, The volumetric flow rate within the core was determined as the ratio of the mass flow rate to the density of the liquid at run temperature,

D. PRESSURE DROP MEASUREMENT

Constant pressure drop was also used as a criterion for onset of steady state, Because the upstream pressure was fixed by the accumulator within a narrow range, a trial-and-error procedure was used in order to match the flow rate nith the corresponding pressure drop. First, the pressure drop was adjusted with the backpressure valve to as high a value as the transducer plate would allow in order to obtain maximum accuracy. Then, the flow rate was adjusted to the proper value by changing the dial of the pump, If the pressure drop increased, the flow rate was reduced, and vice versa, until no more change was observed. No more than three successive adjustments were required usually to reach a constant flow rate and constant pressure drop. A shut-off valve on each of the transducer lines made it possible to change the transducer plate at any time, without having to drop the liquid pressure.

E. MEASUREMENT OF OIL VISCOSITY AT ELEVATED TEMPERATURES

As explained in Paragraph A, a capillary tube tupe viscometer was constructed. It consisted of a 60-inch-long piece of 316 stainless steel tubing with a nominal I.D. of 0.033 in.

The tubing was coiled into a double loop, about 10 inches in diameter, so that it would. fit inside the oven. The flow system was the same as the one represented in Fig.2, except that the core holder was replaced by the capillary tube ana the confining pressure line was not used.

Laminar flow of liquids through circular conduits obeys Poiseuille's law, which can be written:

$$q = \frac{\pi r^4}{8} \frac{\Delta p}{\mu L} \qquad (1)$$

where:

q = flowrate of liquid, cm3/sec

r = inside radius of capillary, cm

Δp = pressure drop across capillary, dynes/cm2

μ = liquid viscosity, poises

L = length of capillary, cm

A more convenient form of Poiseuille's law is:

$$q = 4.437 \times 10^7 \frac{r^4}{L} \frac{\Delta p}{\mu} \qquad (2)$$

where q is in $cm^3/sec.$, r and L in inches, Δp in psi. Viscosity can be calculated by measuring the flow rate and the pressure drop:

$$\mu = 4.437 \times 10^7 \frac{r^4}{L} \frac{\Delta p}{q} \qquad (2a)$$

Because the inside diameter of the capillary could not

be measured exactly, and because the ferrules that made the seal at both ends of the capillary slightly reduced the inside diameter, a calibration of the apparatus vias necessary. Mineral oil No.15 was used as a calibrating liquid at room temperature, because three independent measurements yielded the same value of oil viscosity at room temperature (Ostwald viscometer, Brookfield electroviscometer, and Davidson's [19] data) namely:

$$\mu = 158 \text{ cp at } T = 73^{\circ}F.$$

With this value of the viscosity, it was found that:

$$\mu = 0.05194 \frac{\Delta p}{q} \qquad (3)$$

which yields, by comparison with Eq.2a, an effective inside diameter of 0.03256 in. Eq.3 is the working equation for the apparatus at 73°F. At higher temperatures, a small correction must be made to the dimensions of the capillary tube, due to thermal expansion.

The linea- coefficient of thermal expansion for 316 stainless steel was found in Ref. [35] as B = 8.9 x 10^{-6} in/in°F. Therefore, the length of the tube at a temperature T is:

$$L_m = \left| 1 + B\,(T - 73) \right|$$

and similarly:

$$r_T^4 = r_{73}^4 \left[1 + B\,(T - 73) \right]^4$$

Therefore:

$$\frac{r_T^4}{L_T} = \frac{r_{73}^4}{L_{73}} \left[1 + B\,(T - 73)\right]^3$$

Because the value of B is small, the preceding equation can be approximated by:

$$\frac{r_T^4}{L_T} = \frac{r_{73}^4}{L_{73}} \left[1 + 3B\,(T - 73)\right]$$

Therefore, the working equation for the apparatus at any temperature is:

$$\mu_T = 0.05194 \left[1 + 2.67 \times 10^{-5}\,(T - 73)\,\frac{\Delta P}{q}\right] \quad (4)$$

Eq. 4 was used for calculating the viscosity of White Mineral Oil No.15 at several temperatures ranging from 73°F to 300°F and under an average pressure of about 200 psi, in order to have nearly the same pressure and temperature conditions as for the oil permeability measurements. The Reynolas numbers for these experiments ranged from 0.3 to 25, and because the critical value is 2,000, the flow was always viscous.

The data and results obtained are presented in Table 1 and plotted on Fig.7. As can be seen, close agreement with the data published by Davidson [19] was found.

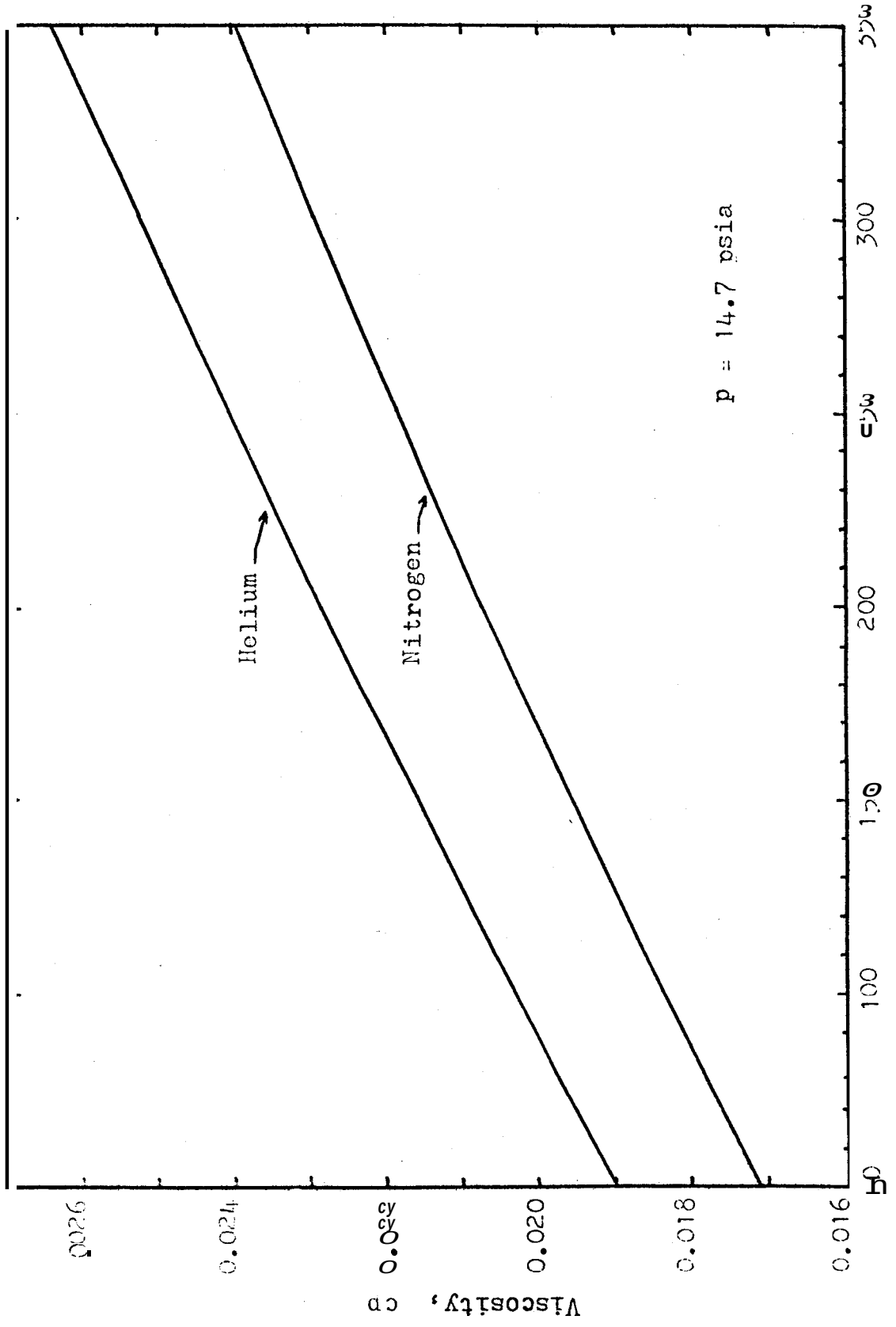

Figure 8. Viscosities of Nitrogen and Helium vs. Temperature.

V. ANALYSIS OF RESULTS AND DISCUSSION

1. WATER FLOW

The first series of experiments was conducted with water saturated cores. Because the primary objective was to isolate temperature as a factor influencing permeability, confining pressure was first held at a constant value while temperature was varied, Then, in a second series of runs both temperature and confining pressure were varied and their combined effect on permeability was observed. Whenever changes in the flow properties were evident, reversibility of the phenomena observed was studied, in an attempt to study any possible hysteresis,

A. EFEST O? TDIPERATURE ON PERMEABILITY AT MODERATE, CONSTANT CONFINING PRESSURE

A constant confining pressure of 2,000 psi was hela on the samoles *is* this preliminary investigation. Results for a Boise sandstone and two Berea sandstones are shown in Figs.9, 10 and 11; they are all similar, and show an important permeability reduction at high temperature. Between room temperature and 300°F the original permeability decreased by 62% for the Boise core No.7, 43% for the Berea core No.12 and 39% for the Berea core No.16. These three cores had been fired once only and stored in distilled water for several months prior

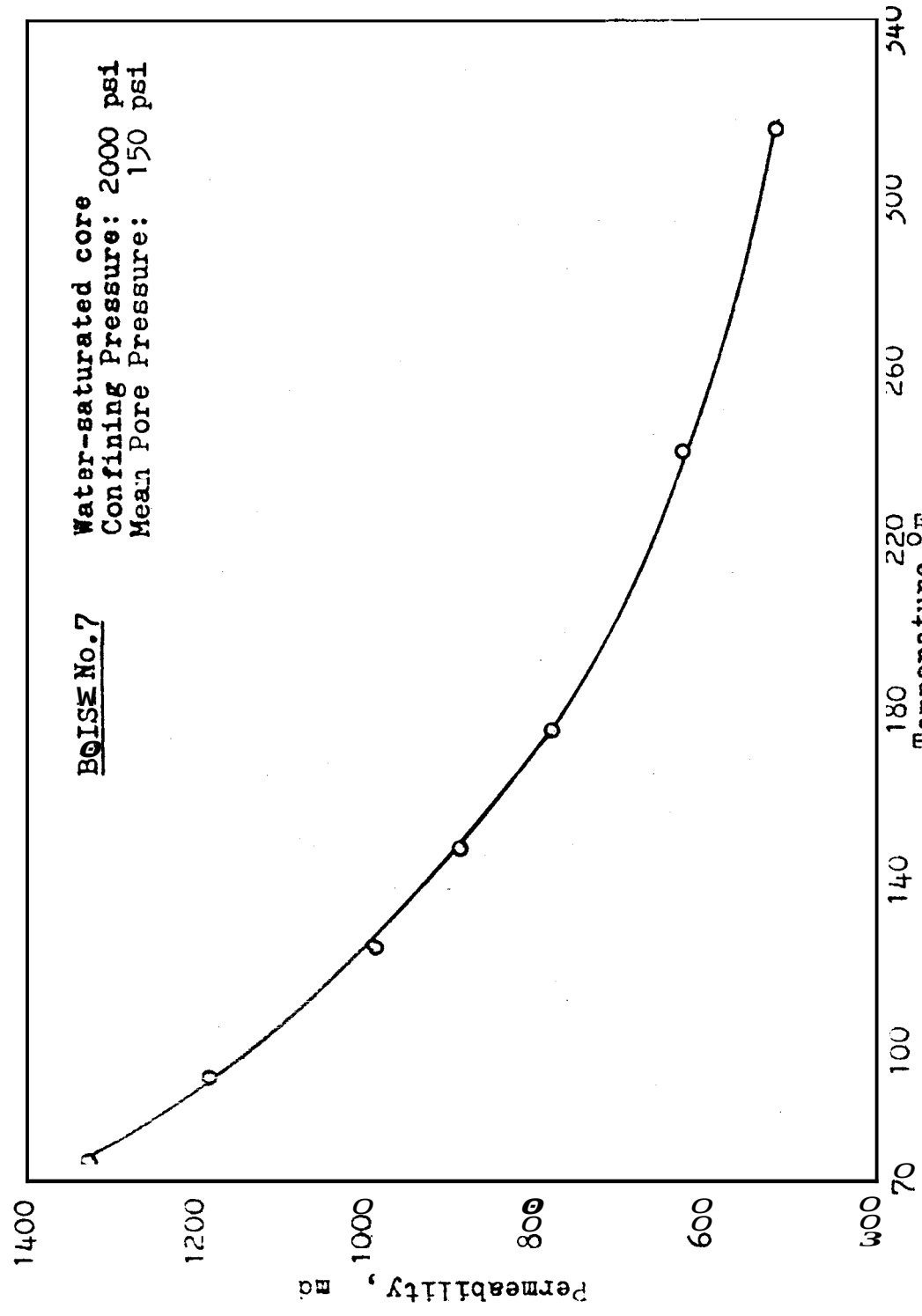

Figure 9. Water Permeability Versus Temperature, Boise Core No.7

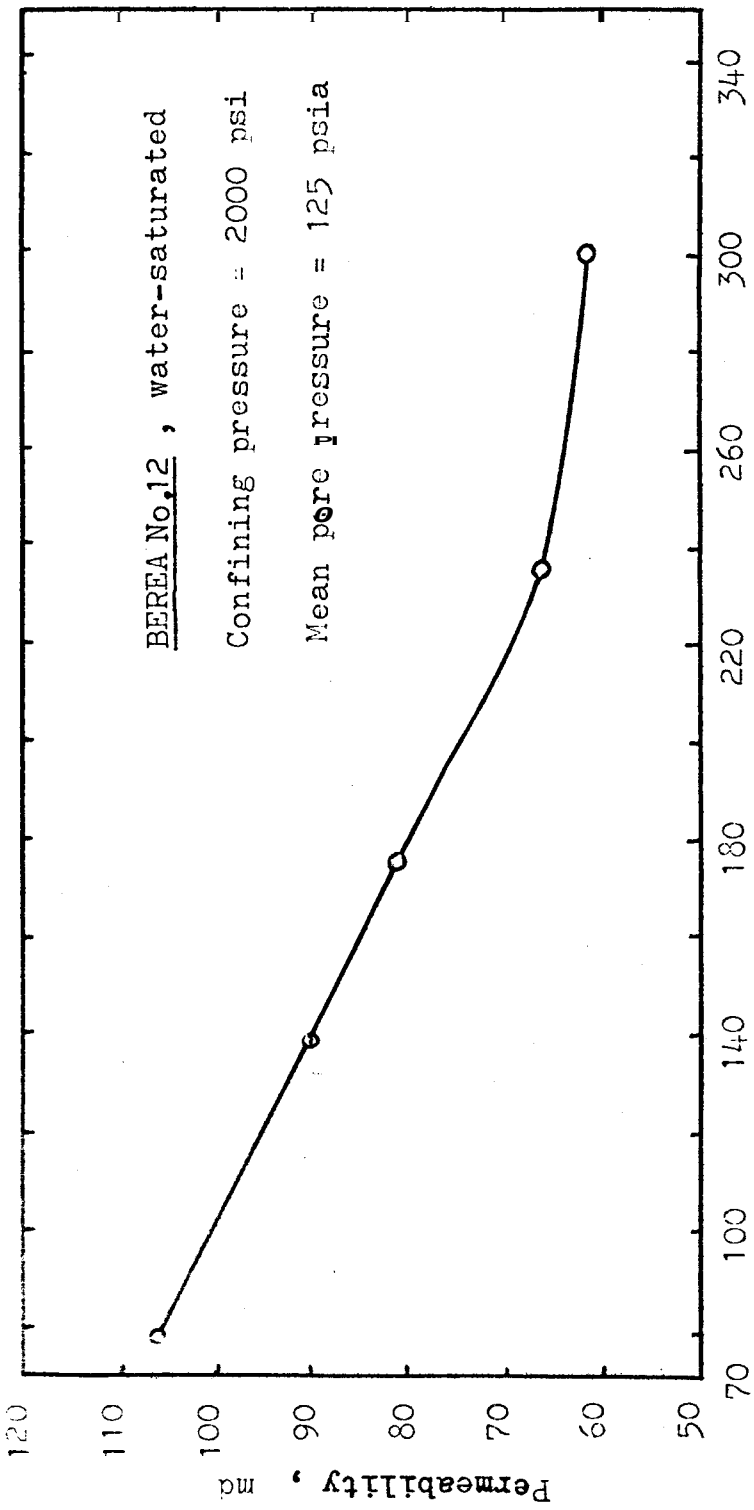

Figure 10. Water Permeability versus Temperature, Berea Core No. 12

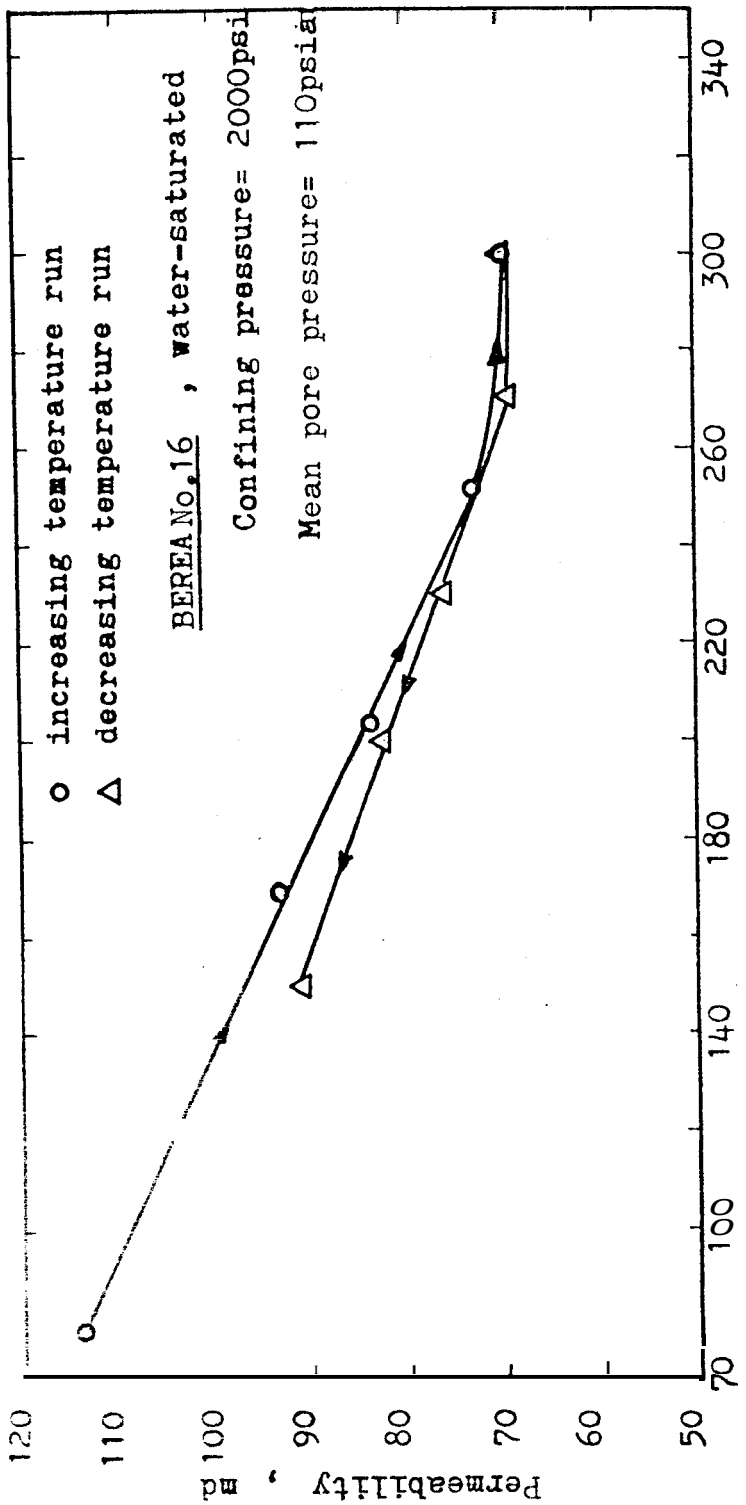

Figure 11 . Water Permeability versus Temperature, Berea Core No.16

to these runs, whereas all the other samples used in this work were fired a second time and stored in distilled water for a few days only.

The preceding results agree qualitatively with previous findings of Weinbrandt (1) who reported as much as 60% reduction in absolute permeability to water between room temperature and 175°F, and of Greenberg, et al. (5) who found as much as 20% reduction in some cases between 80°F and 140°F, for artificially consolidated cores. It should be noted that Greenberg, et al. found no changes in permeability in several cases and an increase in two cases.

Afinogenov (6) used oil to measure permeability and also found a decrease in permeability (up to 95%) between room temperature and 200°F. He attributed this change to a possible reduction in the open spaces of the pores with increasing temperature, or to a change in the physicochemical properties of the liquid as it reacts with the rock minerals with rising temperature. Greenberg attributeu the changed to microstructural rearrangements in the matrix geometry.

Because of the lack of consistency of the published works from both a qualitative and a quantitative standpoint, there is not enough evidence at this point to aecide whether the observed decrease in absolute permeability with temperature increase was cue to purely mechanical action, or to rock-fluid interaction at the surface of the rock, or even to a combination of both effects. Auditional clues will be provided in the following sections by analyzing the data obtained with saturating

fluids other than water at various confining pressure levels.

B. COMBINED EFFECT OF TEMPERATURE AND OVERBURDEN PRESSURE

The value of 2,000 psi for the confining pressure that characterized the results of the previous section, was considered to be only "moderately high", even though it is representative of actual reservoir conditions and has been commonly used in laboratory work on flow properties of rocks. However, much higher values (up to 15,000 or 20,000 psi) have been used by other investigators in somewhat similar work[6,8,11]. The equipment used in the work reported here is rated at 5,000 psi at 350°F safely, but a maximum of 4,000 psi and 300°F was actually used, and proved to be sufficiently high for yielding significant data in most cases.

For the Berea core No.17, the effect of temperature on permeability was investigated at various levels of overburden pressure, ranging from 450 to 4,000 psi. The net confining pressure, defined as (Absolute Overburden Pressure - 0.85 x Pore Pressure) was about 160 psi lower than the overburden pressure. The confining pressure was carefully maintained at each selected level while heating up. The results are presented in Fig. 12 and Table 9. They are similar to those presented in Figs. 9, 10 and 11 in that absolute permeabilities consistently decrease with increasing temperature; but the curves obtained are concave down, whereas they were concave

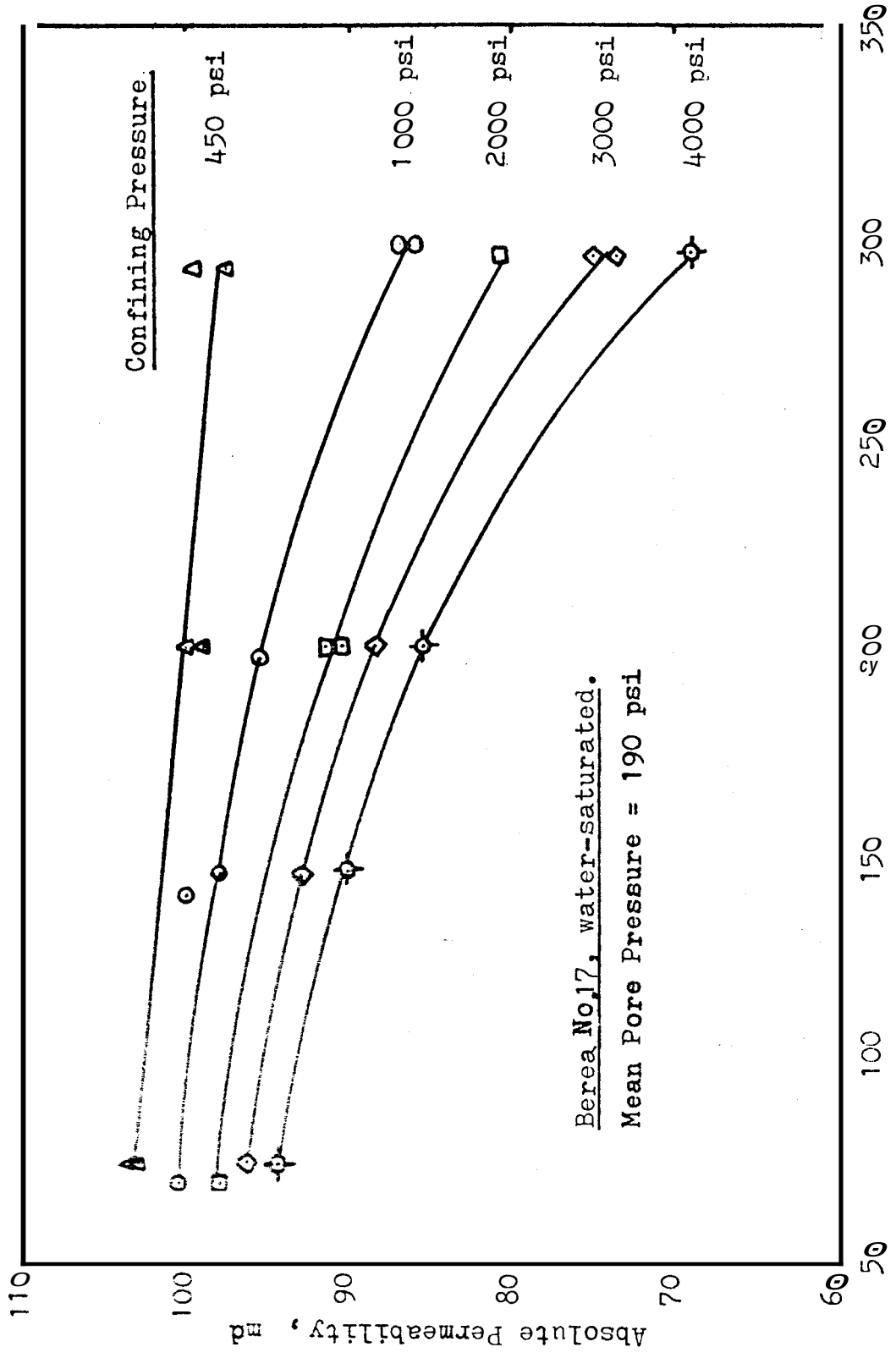

Figure 12. Permeability Change with Temperature and Confining Pressure.

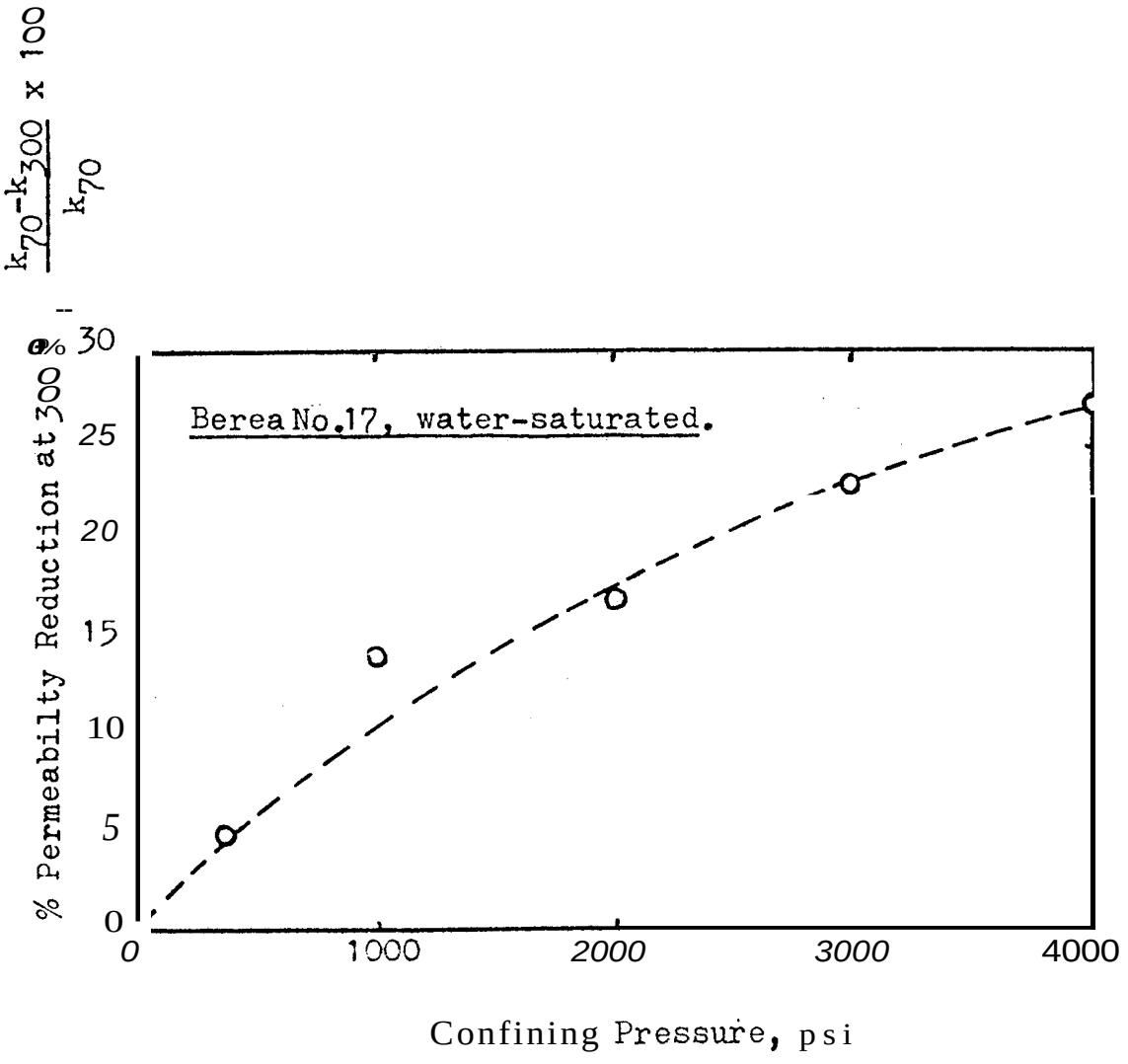

Figure 13. Percentage of Retained Permeability at 300°F vs. Confining Pressure.

up for the first results, This difference in shape may have been caused by the additional firing cycle to which the Berea core No.17 was subjected, or perhaps simply by the nature of the core itself.

Further examination of Fig.12 shows that the effect of temperature is also a function of the overburden pressure. At the low confining pressure of 450 psi the percent decrease in permeability over the entire temperature span is less than 5%, whereas the decrease in permeability is almost 27% at 4,000 psi confining pressure. The percent decrease at 300°F vs. confining pressure has been graphed in Fig.13. It appears that the phenomenons causing the permeability reduction at high temperature and moderate confining pressure, whether mechanical or physicochemical in nature, is intensified by the effect of overburden pressure, Clearly, mechanical stresses play an important role in the .phenomenon observed. By further reducing the pore openings, mechanical stresses accentuate the effect of thermally-induced mechanical stresses. The results at loa values of the confining pressure suggest that thermal stresses acting alone may not cause significant changes in the configuration of the pores and hence in permeability. Perhaps in the absence of external stresses, the rock matrix expands freely under the action of thermal stresses without appreciable changes in the shape of the pores. But in the presence of high overburden pressure, large external forces on the rock matrix will tend to augment the internal stresses, and may cause the formation of "tight necks",

thus decreasing permeability. This observation also implies that the initial condition of the rock is determining as far as the nature of the changes to be expected and the magnitude of these changes. The term "initial condition" mainly refers here to the effective average pore size of the rock at room temperature and low confining pressure, i.e., the average pore size available for flow before any stresses are supplied. Moreover, it is reasonable to believe that the onset of the temperature dependence mill only be observed after the rock has been subjected to a "minimum level of stress", defined by a combination - not necessarily unique - of mechanical and thermal stresses. The possibility that this combination may not be unique is suggested by the analogy between thermal and mechanical stresses.

The minimum level of stress obviously depends on the initial conditio? of the rock as previously defined, which in turn is a function of the nature of the rock and, as will be seen later, of the fluid floc-ing through it. The difference of magnitude in the changes observed with the Boise and Berea sandstones substantiate this theory, At the limit, one would expect certain types of cores to exhibit no temperature dependence under conditions similar to those previously describeu. And indeed results from Arihara [36] show that aqueous permeability of an artificially consolidated core under relatively low confining pressure did not change as temperature increased from 75 to 300°F, which indicates that the minimum level of stress had not been reached. The large changes reported by

Afinogenov [6], on the other hand, seem to indicate that the minimum level of stress had already been exceeded at initial conditions.

C. HYSTERESIS

Because portions of the changes in permeability observed were probably caused to some extent by micro-reorganization of the matrix structure, some degree of hysteresis was to be expected, However, it mas found that in most of the cases studied, the mechanical stresses were moderate enough for the deformations to be essentially elastic. Only at the higher values of both mechanical and thermal stresses did plastic (permanent) deformations occur to a significant degree.

An easy check on whether or not permanent deformations had occurred was performed by re-measuring the room temperature permeability after allowing the system to cool. After the heating cycle the permanent reduction in permeability was typically 1 to 3% at low to moderate values of the confining pressure, Fig.11 shows a typical increasing-decreasing temperature run for the Berea core No.16. As can be seen the results show only a small permanent change and were essentially reversible.

A special investigation of hysteresis was made with the Boise core No.2. Fig.14 shows the effect of temperature at 700 psi and 3,700 psi net confining pressure, respectively. In both cases, room temperature permeability following the heating cycle was measured and is shown on the same graph, There was only a 3% permanent loss in permeability at loa confining pressure,

whereas there was almost a 20% decrease at high confining pressure, At this high value of the confining pressure, the core was then subjected to four additional heating and cooling cycles, between room temperature and 300°F. The results of this series of runs are presented in Table 2, App.A. It appears that a large permanent drop in permeability(20%) happened during the first cycle, During the following cycles, the percentage of retained permeability loss at room temperature was of the same order of magnitude, 2 to 3%. The percentage of permeability reduction due to thermal stresses appears to be reasonably constant from cycle to cycle, ana the value of 24 to 35%, even though smaller than the value obtaineo with Boise core No.7, indicates a definite temperature dependence.

D. EFFECT OF CORE FIRING TEMPERATURE

In an attempt to reproduce the results presented in sub-section A for the Boise core No.7, and to extend them to various confining pressure levels, this core was extracted and placed in the furnace for ignition, according to the program that was described in Section IV-1 on Core Preparation. But the sample was accidentally heated for several hours at temperature close to 1,400°F (760°C), i.e., at a temperature well in excess of the recommended 500°C. Somerton, et al.[917] showed that heating sandstones to temperatures in this range can cause enough structural damage to double the original permeability, Their results were obtainea with Bandera,

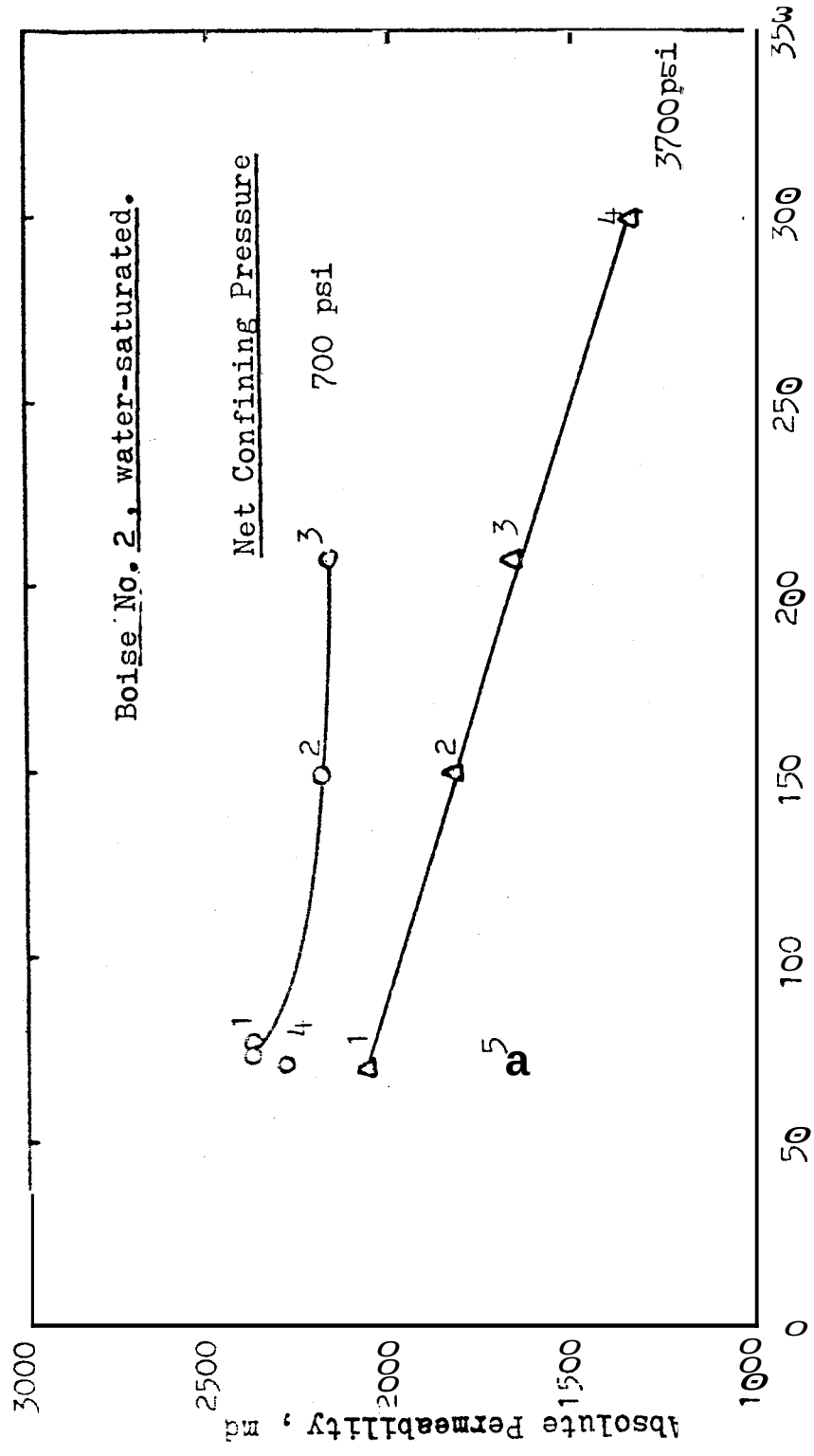

Figure 14. Permeability versus Temperature for Boise Core No.2

Berea and St. Peter sandstones respectively, By analogy, similar behavior should be expected with Boise sandstone, and, indeed, the aqueous permeability of the Boise core No.7 after ignition at 760°C was found to be 1852 md at room temperature and 2,000 psi confining pressure. This is 39% larger than the permeability measured under the same conditions after ignition at only 500°C (see Fig.9).

The important point is that this change in the initial firing treatment of this core drastically changed its high temperature behavior. The combined effect of thermal and mechanical stresses was investigated in the ranges 70-210°F temperature and 1,000-4,000 psi confining pressure. The results are shown in Fig.15. The percentage of permeability reduction never exceeded 3 to 4%, as opposed to a reduction of approximately 50% for the same temperature span before thermal alteration had occurred (see Fig.9).

These interesting results indicate that the initial firing of the core may be even more important in the temperature dependence of permeability than the combination of thermal and mechanical stresses.
A detailed analysis of the factors influencing the initial condition of the core will be presented in Section V.4. But first the results of the experiments conducted with fluids other than water will be presented in Sections V.2. and V.3.

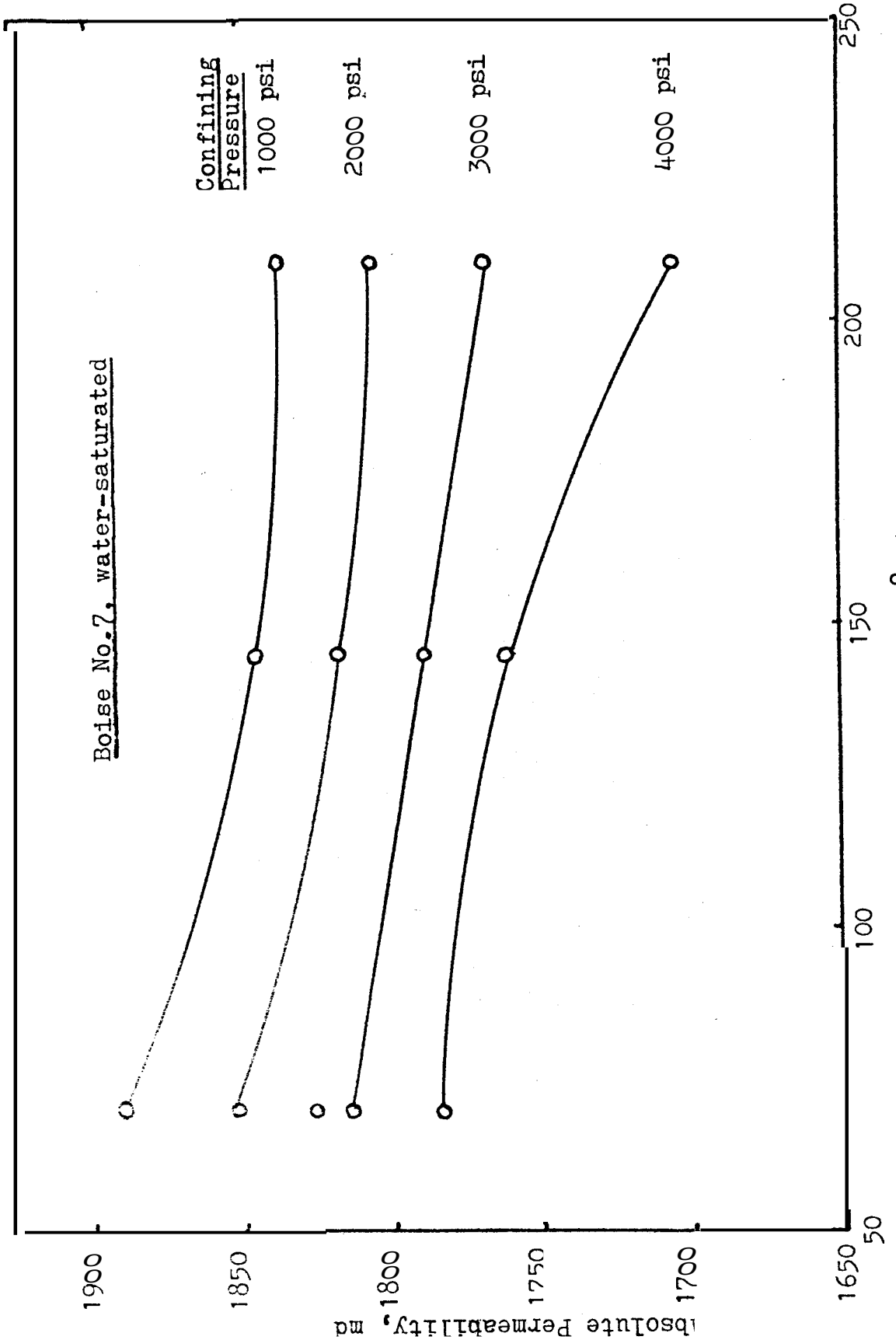

Figure 15. Permeability versus Temperature for Boise Core No.7 after Firing at 760°C

2. GAS FLOW DATA

In the light of the results obtained with water flow, the speculation was originally made that thermally-induced mechanical stresses were the main cause for the permeability decrease at high temperatures, and that there might be an apparent porosity reduction accompanied by some kind of fluid entrapment. As a result of this speculation, gas flow experiments were originally designed to permit detection of the existence of potential entrapment, and hopefully measure the amount of fluid entrapped. The method was to flow an inert gas (such as nitrogen) through the rock sample, and elevate the temperature, perhaps causing entrapment of some of the nitrogen within the rock. Then another inert gas, e.g., helium, would be allowed to flow for some time. Then flow would be stopped and the system would be allowed to cool down. Finally, resumption of helium flow should sweep out any nitrogen entrapped at high temperature, The nitrogen would be detected by continuous analysis of the effluent gas, A gas analyzer having an extremely sensitive thermal conductivity cell was selected for that purpose,

A. EFFECT OF TEMPERATURE ON EXTRAPOLATED PERMEABILITY AT CONSTANT CONFINING PRESSURE

The first series of gas flow experiments was conducted on the Bandera No.29 core at a constant confining pressure of 2,000 psi. Details on the analysis of gas flow data are given in Appendix B. Apparent permeabilities were measured

with nitrogen under conditions of viscous flow at five different temperatures and graphed as a function of the reciprocal mean pressure on a conventional Klinkenberg graph. Fig.16 shows that this resulted in five different straight lines, which intersect the infinite mean pressure line ($\frac{1}{p_m} = 0$) at the same value of 35 md. This "extrapolated permeability" represents the fluid-independent absolute permeability of the rock. Therefore, according to Fig.16, the absolute permeability of the Bandera No.29 core remained constant at all temperatures.

Similar results were obtained with two more rock samples. Fig.17 shows the data obtained with the Berea core No.12. The confining pressure was also 2,000 psi, and the extrapolated permeability showed a slight increase from 141 to 143 md with temperature. This value of the absolute permeability is about 35% higher than the value that was measured with water at room temperature under the same confining pressure (see Fig.10). Potential reasons for this difference will be given in Section V.4., and will provide a clue as to the cause of temperature having a different effect depending on the fluid that saturates the rock.

Fig.18 shows similar results for the Berea core No.16. The confining pressure was only 600 psi. A constant extrapolated permeability of 133 md was measured at all temperatures. In order to check the results obtained with nitrogen, the permeability of the Berea core No.16 was also measured with helium, at 66°F under 600 psi of confining pressure (see Fig.19).

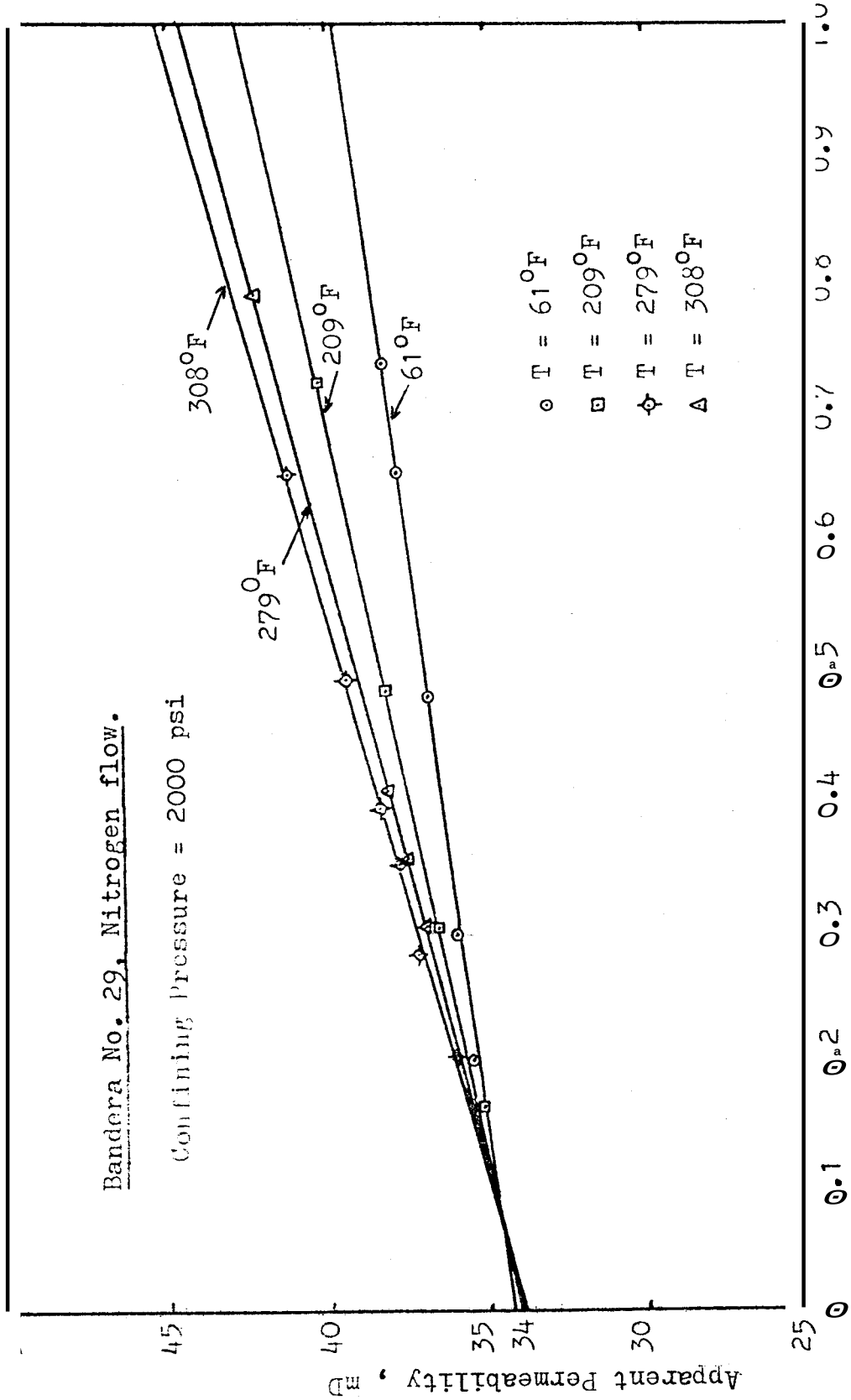

Figure 16. Klinkenberg Permeability versus Reciprocal Mean Pressure at Several Temperatures for Bandera Core No.29

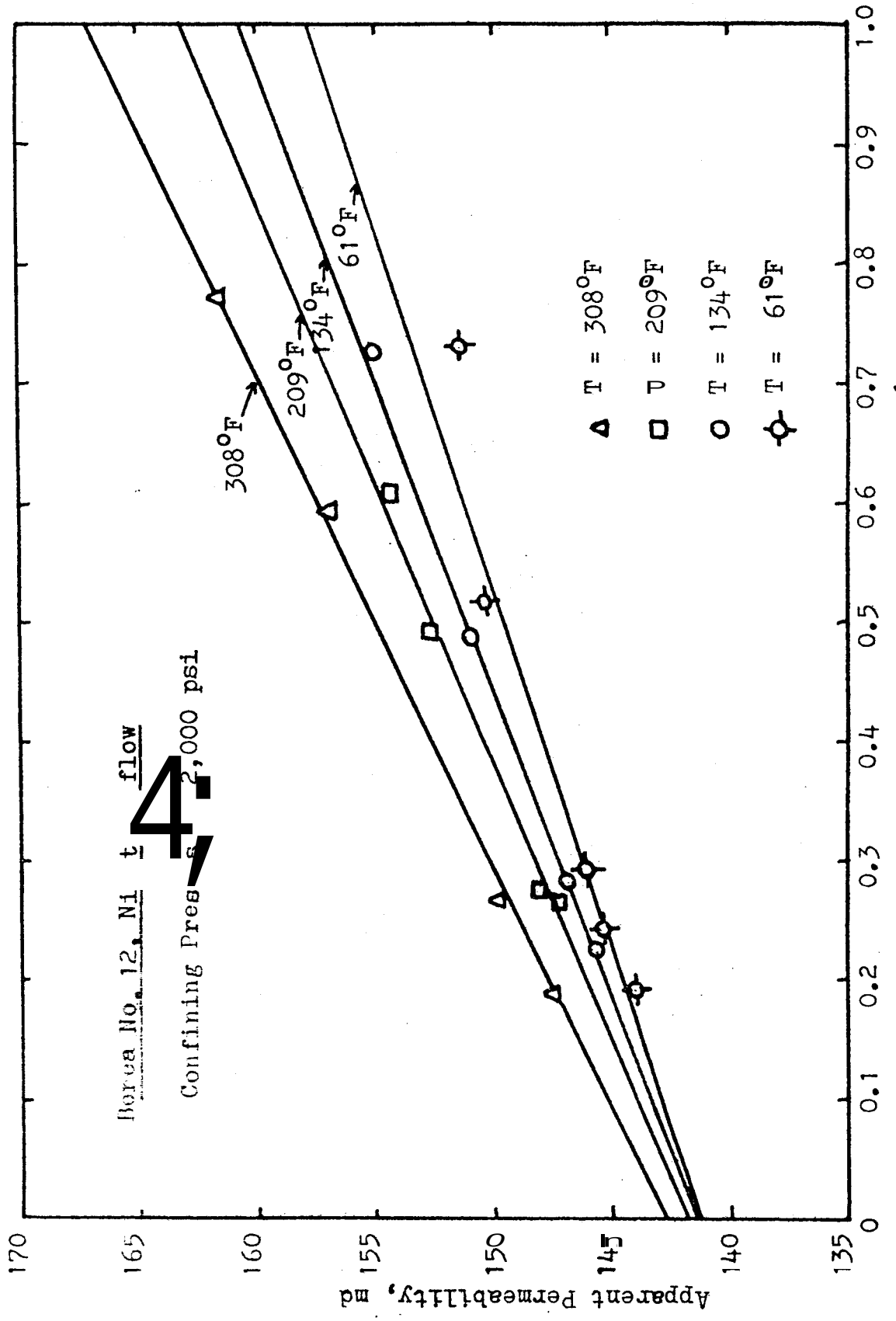

Figure 17. Klinkenberg Permeability versus Reciprocal Mean Pressure at Several Temperatures for Berea Core No.12

A Klinkenberg line of higher slope resulted, but an extrapolated permeability of 132 md was obtained, i.e., a value almost identical to that measured with nitrogen. Again, this value was significantly higher than the corresponding water Permeability of 114 md at room temperature and 2,000 psi confining pressure (see Fig, 11). Because the difference in confining pressure alone cannot explain such a change in permeability (see Fig.12), it may be concluded that rock-fluid interaction is largely responsible for the unique thermal behavior observed with the water-saturated Berea core No.16. This point will be explored further in Section V.4.

B. EFFECT OF TEMPERATURE ON THE KLINKENBERG SLIP FACTOR

A definition of the Klinkenberg slip factor "b" is given in Appendix B. Graphically, b is easily determined from the slope of the straight lines obtained on conventional Klinkenberg graph6 (Figs.16, 17 and 18).

If k_{max} is the apparent permeability extrapolated to atmospheric mean pressure and k_{∞} the permeability extrapolated to infinite mean pressure, then the b factor is given by:

$$b,\ atm = \frac{k_{max} - k_{\infty}}{k_{\infty}}$$

It is generally acknowledged that b is a constant for a given porous medium [38]. However, as indicated in Appendix B, this is only true at a given temperature, According to Eq. B-4 in

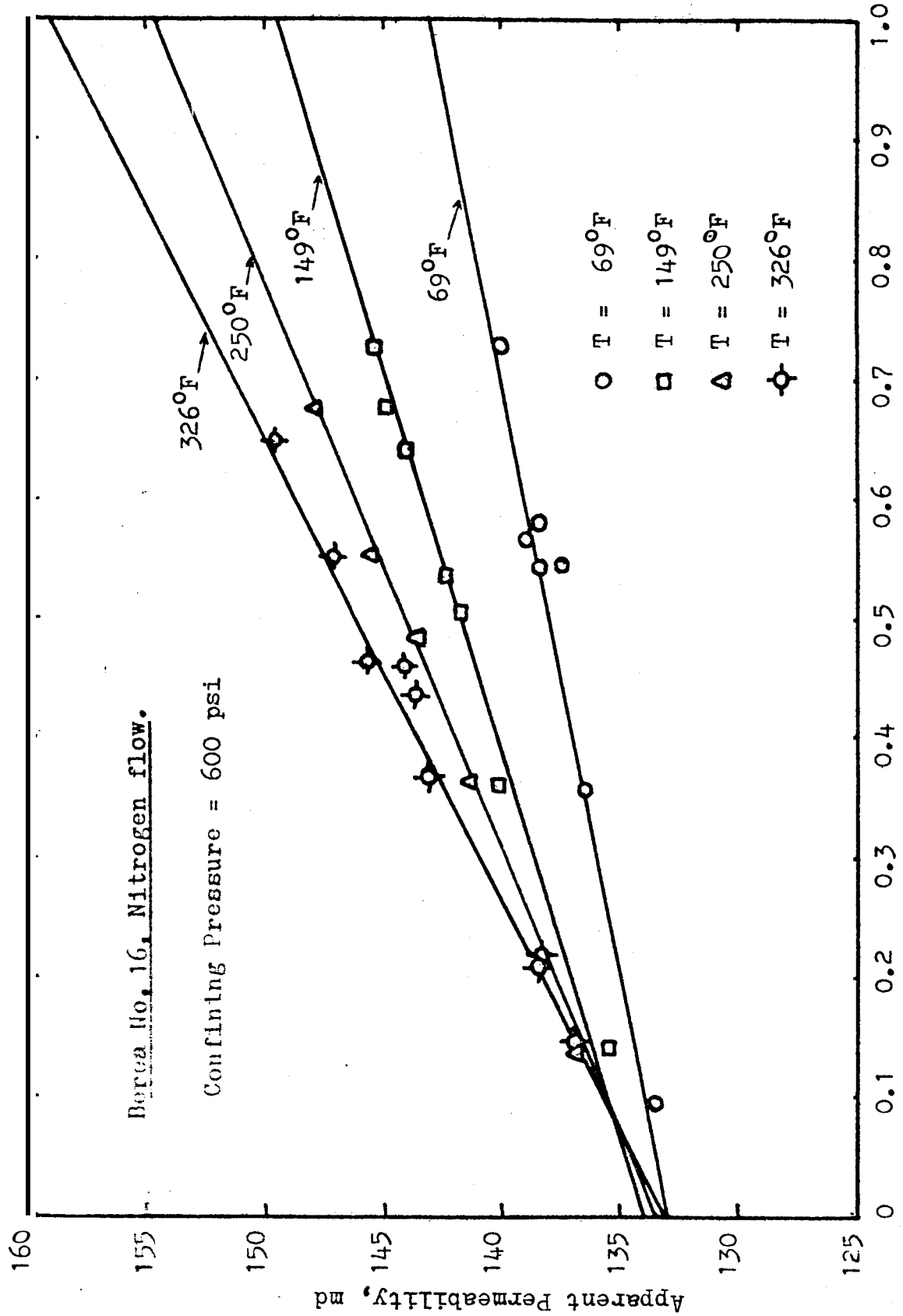

Figure 18. Klinkenberg Permeability versus Reciprocal Mean Pressure at Several Temperatures for Berea Core No.16

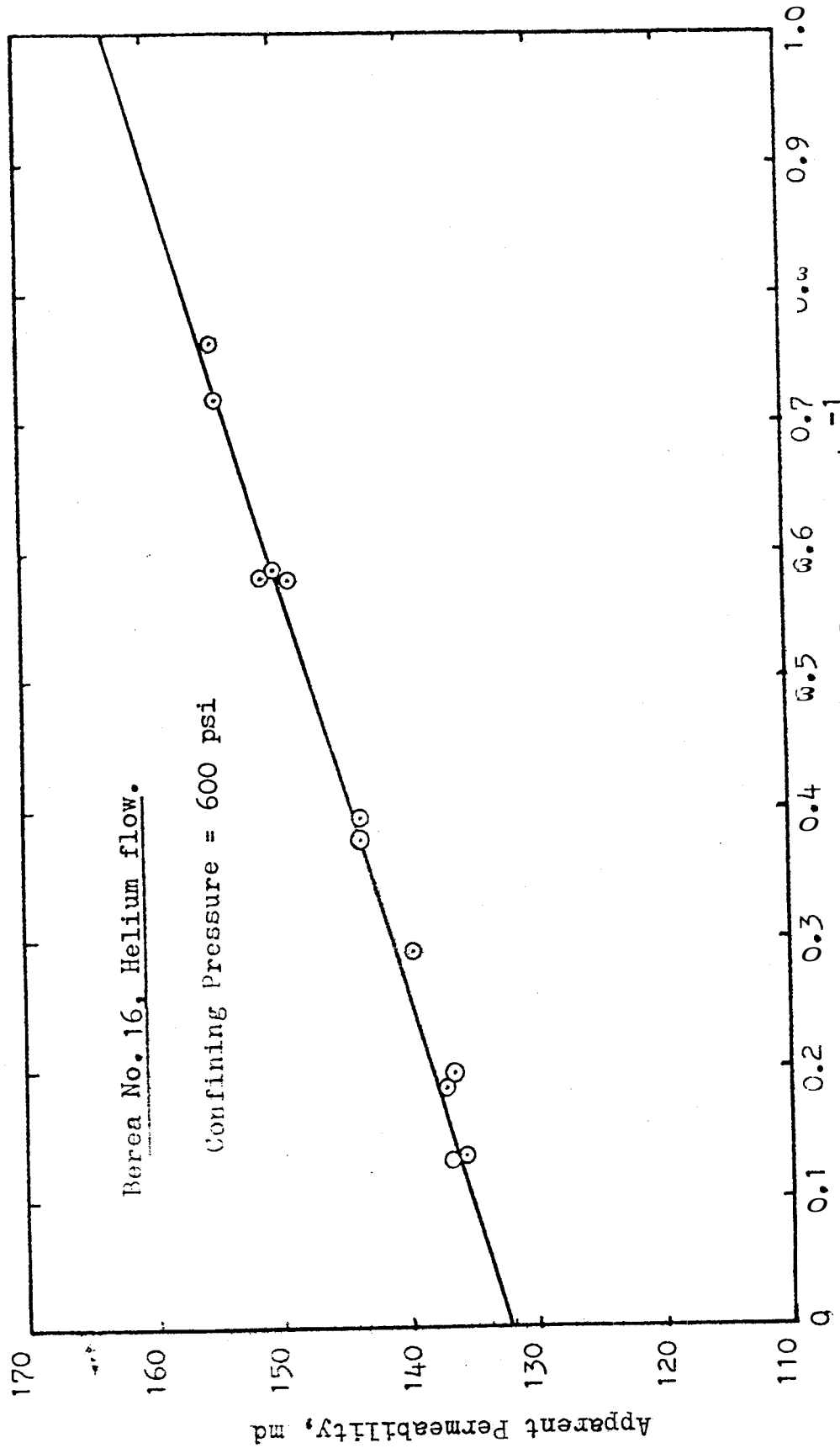

Figure 19. Klinkenberg Permeability at Room Temperature, 66°F
for Berea Core No. 16 with Helium Flow

Appendix B, be should be directly proportional to temperature, The values of b were calculated from the Klinkenberg straight lines for Figs.16, 17 and 18, respectively, converted into psia, and graphed versus temperature (in ^{o}R) on the same graph (see Fig.20). As can be seen, the Klinkenberg slip factor varied linearly with temperature for the three rock samples studied. However, the direct prouortionality predicted by theory was not found, The room temperature values of b are in good agreement with the following general correlation proposed by Jones (39) :

$$b, psi = 6.9\ k^{-0.36}$$

The values measured experimentally and the predicted values are shown in the following table:

Core No.	k, md	b, psi measured	b, psi correlation	% error
Bandera No.29	34	2.22	1.94	-12
Berea No.12	144	1.70	1.15	-32
Berea No.16	133	1.10	1.19	+7

C. ANALYSIS OF VISCO-INERTIAL FLOW DATA

According to the methods describe6 in Appendix B, two kinds of data were obtained. When a large amount of backpressure was

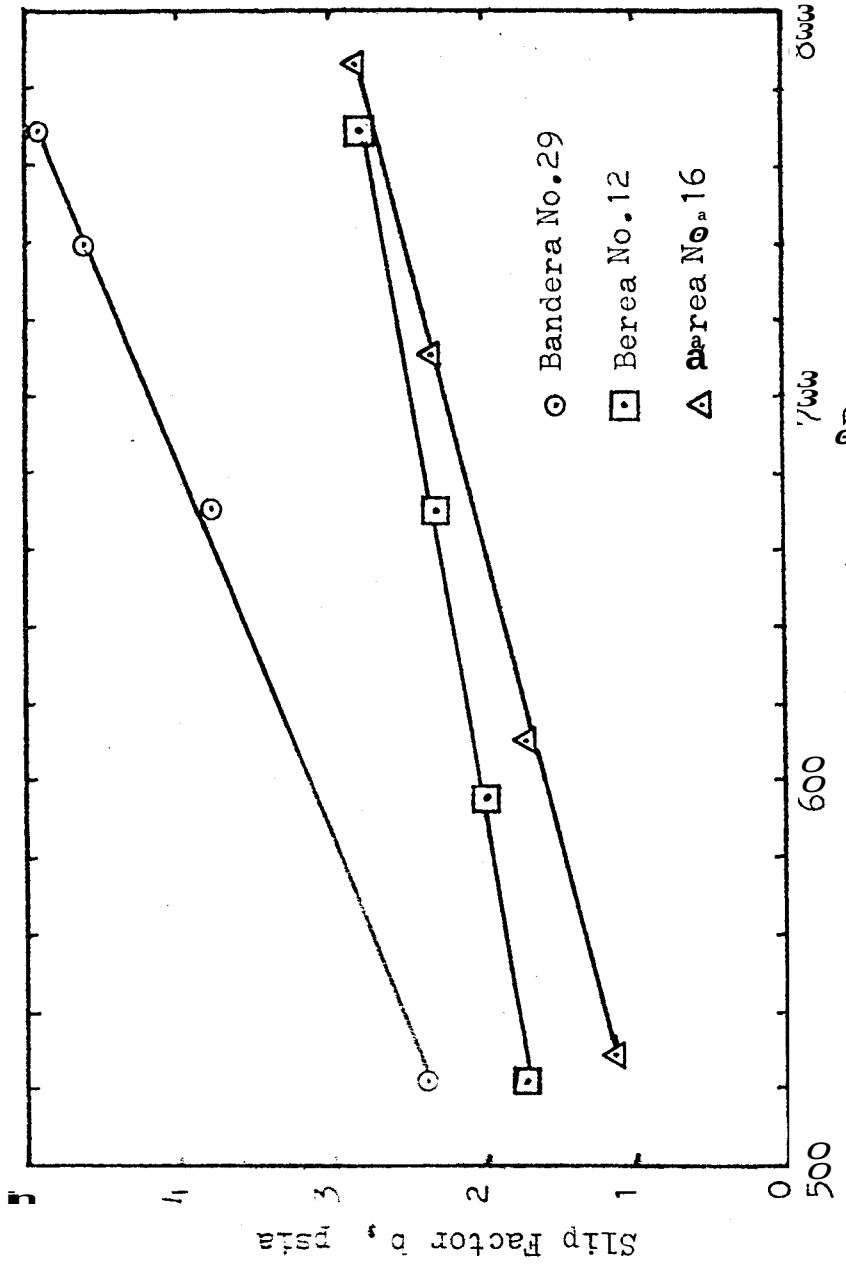

Figure 20 . Effect of Temperature on Klinkenberg Slip Factor, for Nitrogen Flow

applied, the flow was viscous and a Xlinkenberg straight line could be obtained. By gradually releasing the backpressure, turbulent flow vias initiated and for a given mean pressure the permeabilities measured were much lower than the Klinkenberg permeability corresponding to that particular mean pressure. Fig.21 shows a typical set of data for the Berea core No.16 at room temperature. A large number of data points are located in the visco-inertial region. These data points, when analyzed in the manner described in Appendix B, result in a straight line on a modified visco-inertial graph. The slope of this straight line is the turbulence factor β, and the intercept with the Y-axis is the reciprocal absolute permeability. If a good truncation of viscous and visco-inertial data has been made, the absolute permeability resulting from the modified visco-inertial graph should agree with the absolute permeability from a conventional Klinkenberg graph. In the case of Fig.22, for instance, the value 131.9 md is in good agreement with the value 133 md obtained from the Klinkenberg graph (Figs. 18 or 21).

D. EFFECT OF TEMPERATURE ON TURBULENCE FACTOR

The procedure described in the preceding section was applies to the Berea core No.16 at all temperatures and four identical straight lines resulted. Rather than showing four different visco-inertial graphs, the data for all temperatures have been plotted on the same graph (Fig.23) and one can see that this yields a single line of slope $\beta = 9.0 \times 10^{7} ft^{-1}$.

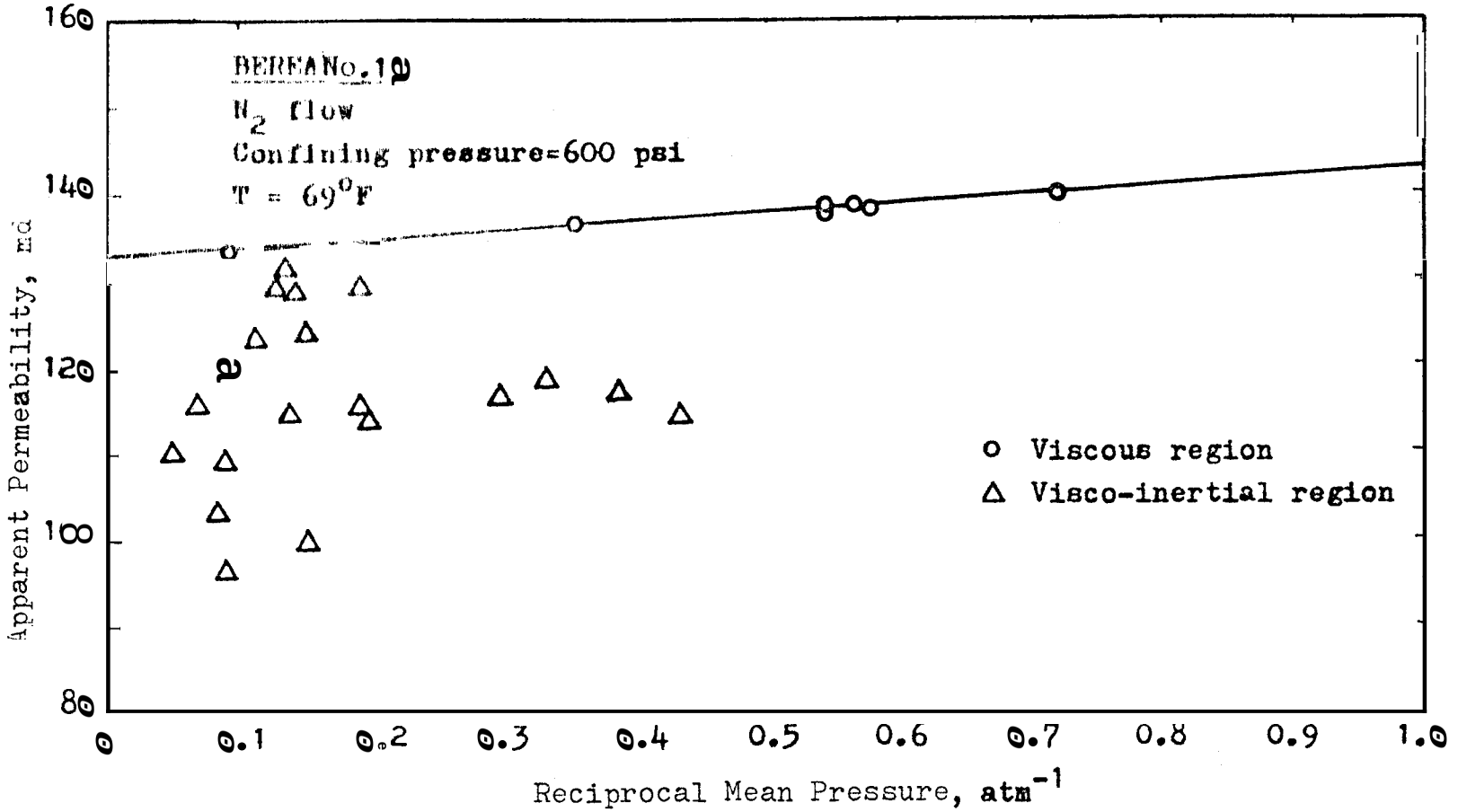

Figure 21. Typical Klinkenberg graph for laminar and turbulent flow, Berea Core No.16, Nitrogen Flow

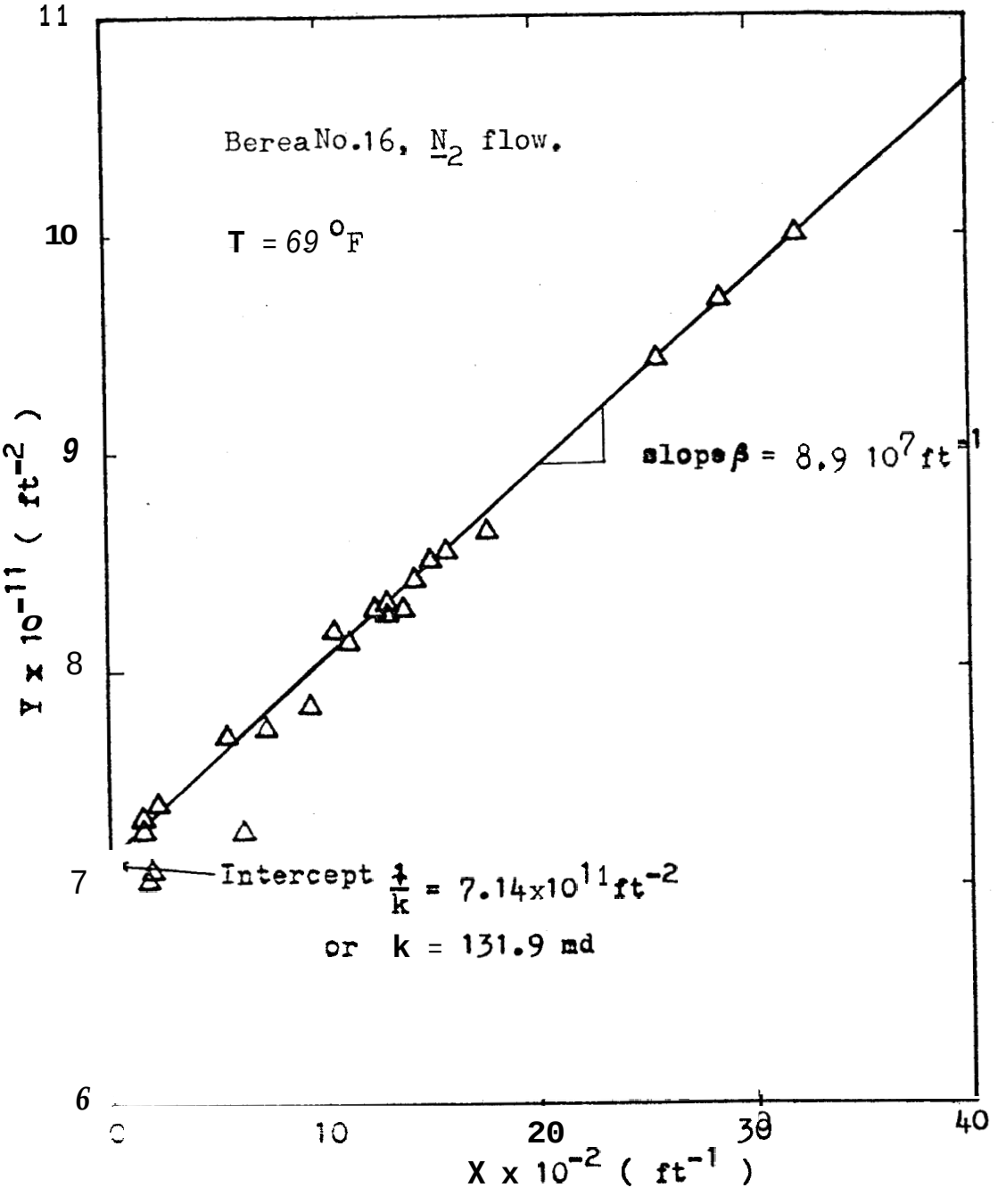

Figure 22. Modified Visco-inertial Graph, Berea Core No. 16 with nitrogen Flow

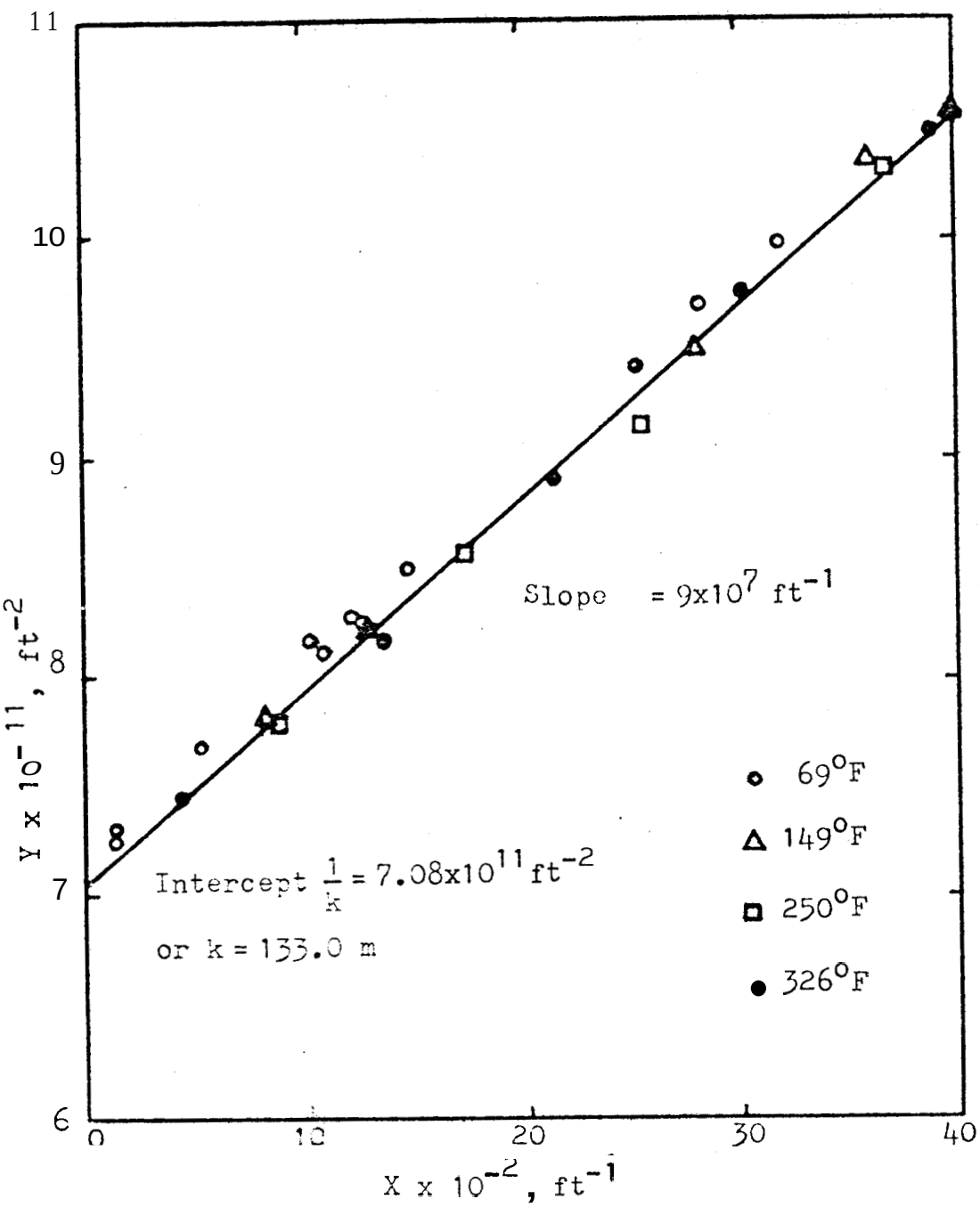

Figure 23. Modified Visco-inertial Graph, Berea Core No.16, with Nitrogen Flow at Several Temperatures

The intercept is:

$$\frac{1}{k} = 7.08 \times 10^{11}\ ft^{-2}$$ which gives k = 133 md as expected.

Therefore, the turbulence factor is independent of temperature. Because correlations involving only the turbulence factor and the absolute permeability have been derived (40), this result was to be expected from the fact that gas permeability remained constant at all temperatures. The above value of β is in excellent agreement with the correlation proposed in ref.40.

3. MINERAL OIL FLOW

Because of the difference between the results obtained at elevated temperatures with water-saturated and gas-saturated cores, it appeared necessary to run similar experiments with another fluid, Apart from the large viscosity and density differences, water greatly differs from gas in that it is a polar fluid which may interact with the rock surface. In order to find out whether surface effects were significant, Chevron White Oil No.15 was chosen for its non-polar characteristics, Fig.5 shows the density of this oil as a function of temperature, while Fig.7 presents its viscosity as a function of temperature.

A. EFFECT OF TEMPERATURE ON PERMEABILITY AT MODERATE, CONSTANT CONFINING PRESSURE

Similar conditions to the water flow or gas flow experiments

were obtained by holding a confining pressure of 2,000 psi around the cores. Two cores were used in this series of runs. Results for the Berea core No.14 are shown on Fig.24, and results for the Boise core No.6 are presented on Fig.25. As can be seen, a slight increase in absolute permeability vias observed, followed by a slight decrease. But these changes barely exceeded the range of experimental error. A horizontal line could have been drawn through the data points. In other words no significant change in absolute permeability to oil was observed with either the Berea or the Boise sandstone, The permeability of the Boise core No.6 was found to be approximately 2,500 md. For the same sample with water flow, Weinbranat (1) reported a decrease from 1,830 to 695 md between 80°F and 175°F. Again, it is interesting to note that the absolute permeability at room temperature was significantly lower (27%) for the water saturated core than it was for the oil-saturated core. The same observation had been made earlier for the gas and water permeabilities of the Berea core No.16 and Berea core No.12. This suggests that the phenomenon causing the permeability reduction of the water-saturated cores at room temperature may also be responsible for the permeability reduction at high temperatures.

B. COMBINED EFFECT OF TEMPERATURE AND OVERBURDEN PRESSURE

Though the previous experimental results gave no indication that absolute permeability to oil would decrease with increasing

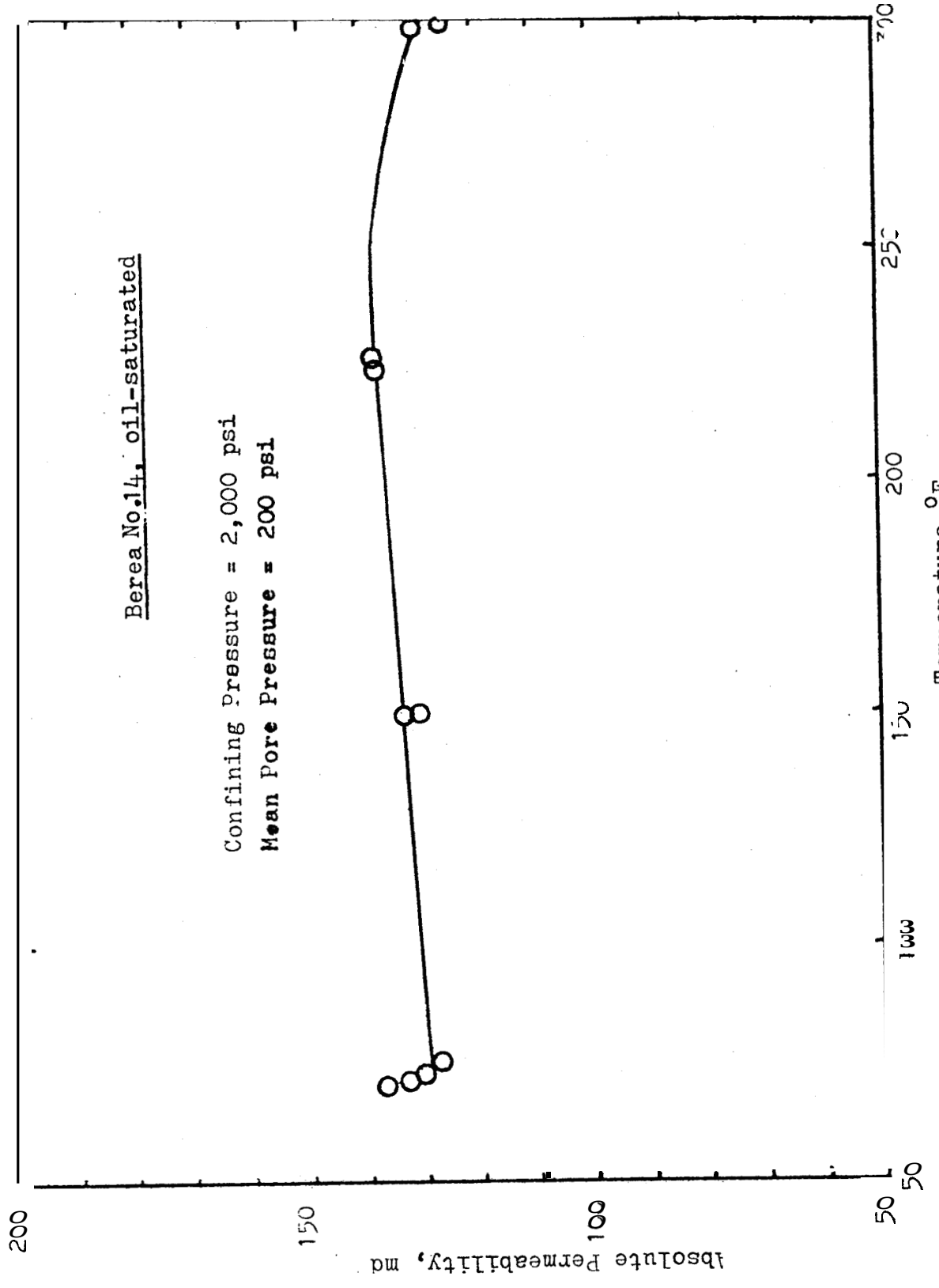

Figure 24. Absolute Permeability versus Temperature for Berea Core No.14 Saturated with Chevron White Mineral Oil No.15

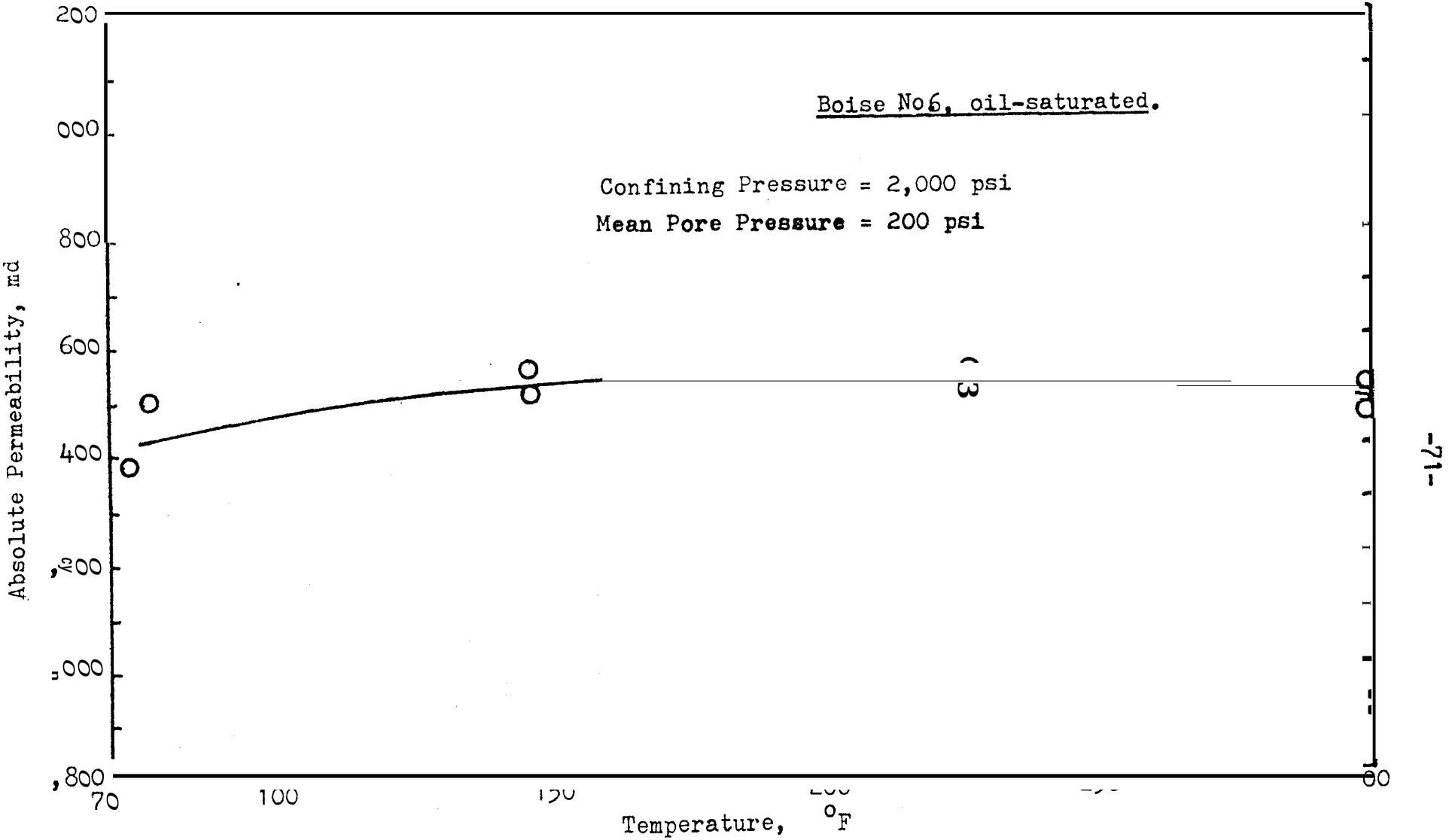

Figure 25. Absolute Permeability versus Temperature for Boise Core No.6 Saturated with Chevron White Mineral Oil No.15

temperature, a series of similar experiments was conducted on the Boise core No.3 at various levels of confing pressure. Results are shown on Fig.26. It is seen that absolute permeability was affected by confining pressure, as expected, but to a lesser degree by temperature, The absolute permeability to oil actually increases with increasing temperature contrary to the water result and previous lack of effect with oil shown in Figs.24 ana 25. For the water-saturated cores, the maximum temperature dependence was observed at the maximum value of confining pressure, i.e., 4,000 psi. Fig.26 shows that, even at such a high confining pressure, thermal stresses were not sufficient to reduce the permeability of the oil saturated core. The absence of rock fluid interaction is believed to be responsible for that behavior. It is interesting, though, that the increase is less at higher confining pressure. In essence, this is the same trend that we observed for aqueous permeability.

4. INTERPRETATION OF THE FLUID DEPENDENCE: CLAY-WATER RELATIONSHIP

Because most reservoir rocks are believed to be water-wet, water has been widely used in laboratory work to measure the flow properties of rocks. Flow of water through porous media is of major importance in many fields, such as ground water hydrology, soil science, reservoir engineering, geothermal reservoirs, etc. In the particular field of reservoir engineering, special interest in the flow of water through porous

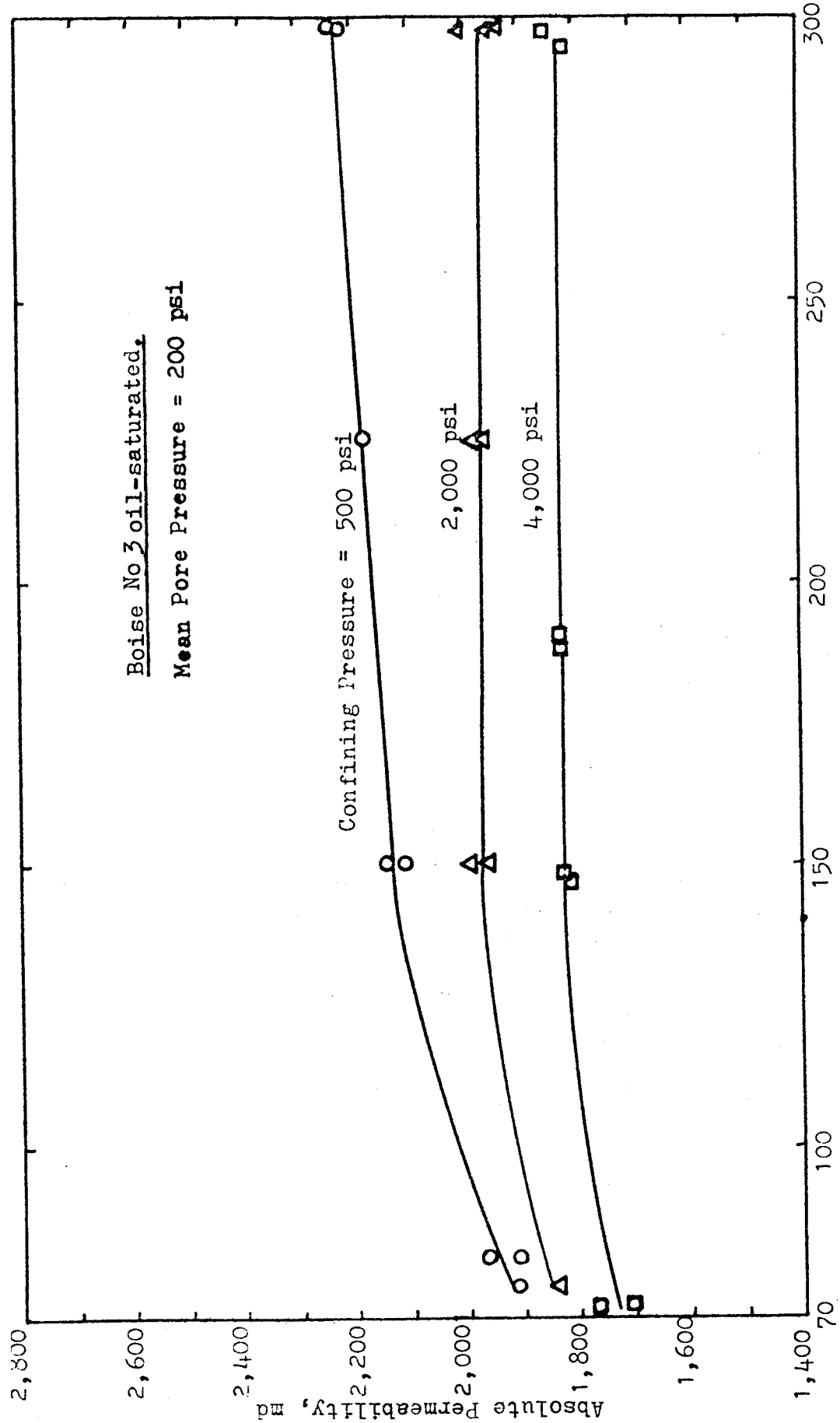

Figure 26. Absolute Permeability versus Temperature and Confining Pressure for Boise Core No.3, Oil Saturated

media is generated by many engineering aspects of oil production, such as water drive, hot or cold water injection, steam drive, coning phenomena, producing water-oil ratio, and many other matters. Therefore, it is essential to know the absolute permeability to water of the rock considered, ana in many cases, the effect of temperature and pressure on this permeability.

However, it has long been recognized that water is not a typical liquid. The problem most commonly encountered in the determination of absolute permeability of water-saturated cores is that of clay swelling. The absorption of water by clay depends upon the kind and the amount of clay minerals present within the rock. For instance, montmorillonite, illite, halloysite and kaolinite are four different types of clay and the amount of swelling that they exhibit decreases in the order in which they were listed.

Appendix C shows the typical mineralogical composition of Boise, Bandera, and Berea sandstones. These three types of rocks contain 34.8%, 21.2% and 19.0% of kaolinite and matrix, respectively. These figures, published by Somerton, et.al.(29), may vary from one sample to another but do provide an order of magnitude for the amount of clay that one would expect to find in these rocks. As mentioned earlier, kaolinite is not a highly swelling clay, as compared to montmorillonite for instance.

Furthermore, the cores used in this work were fired at a a temperature of 940°F, which is generally acknowledged to

oxidize any organic matter and to deactivate swelling clay. Accoraing to Grim [30], who presented a general discussion of the firing properties of various clay minerals, temperatures on the order of 100 to 300°C cause the loss of the ability to swell again. The loss of swelling potential is related to the complete loss of interlayer water; thus, heating must be continued at the required temperature for a considerable time, if the permanent loss of swelling is desired, As a result, one would expect repeated firing cycles to have a cumulative effect on the deactivation of clay, especially if the swelling ability is not totally eliminated by the first cycles. Comparison of the permeability values obtained by Weinbrandt [1] (1,800 md for the Boise core No.6 and 1,620 md for the Boise core No.2) with the values for the same cores obtained in this work (2,500 md for the Boise core No.6 and 2,200 md for the Boise core No.2) do support this conclusion. Both cores were heated to 950°F for more than five hours prior to the runs corresponding to Fig.s 14 and 25. This additional heating cycle caused a significant increase in permeability at room temperature and a reduction of the temperature dependence. But the permeability of the water-saturated Boise core No.2 still decreased with increasing temperature, whereas the permeability of the oil saturated Boise core No.6 remained reasonably constant at all temperatures.

In order to understand the physical phenomena responsible for these opposite effects, we must take a closer look at the actual rock-fluid interaction taking place at the surface of

the rock. First of all, it is important to realize that the key to the surface effects considered here is the unique structure of the water molecule. The hydrogen atoms are deeply imbedded in the oxygen atom so that the molecule is approximately spherical. Its rauius is only slightly greater than that of the oxygen ion, The bond angle between the lines joining the hydrogen nuclei to the center of the oxygen atom is 105°. This structure results in a very uneven distribution of charges in the molecule. An excess of positive charges appears at or between the protons, and the opposite siae of the molecule is negatively charged. Thus the water molecule is a dipole, and this polar character constitutes the key to its unique properties. The oxygen atoms in the clay-mineral surface are definitely organized and consequently there exists a pattern of charges on this surface. The charges pattern can be carried over into the water molecules and favors the development of a definite configuration in the initially adsorbed water.

A comprehensive review of the mechanisms involved in clay-water interaction was presented by Grim [31]. There is general consensus among all investigators that the water held directly on the surfaces of the clay particles is in a physical state different from that of liquid water. Though various concepts have been proposed to explain the actual arrangement of water molecules at the rock surface, it is generally believed that a film consisting of several layers of "non-ordinary" water develops on the flat surfaces of the clay minerals. Many

studies have led to the conclusion that the nature of the initially adsorbed water is quasi-crystalline, i.e., similar to that of ice. Grim quotes numerous investigators who concluded that the inapplicability of conventional flow equations to water movement through clay materials is an indication of an immobile or highly viscous water layer on the particle surfaces, which makes the effective porosity much less than the measured porosity.

Not all investigators agree on the thickness of the adsorbeu nonliquid water and the figures proposed vary for kaolinite from a few molecular layers to several hundred Angströms. However, the experimental results obtained in the present work inuicate that a relatively high level of immobilization of the water molecules actually took place, because permeability reductions of about 30%were observed for the water-saturated cores at room temperature,

The effect of temperature on the cation exchange capacity of clays, and more precisely kaolinite, is important in this work. Unfortunately, little data is available in the literature on this subject. According to Kelley (32) the temperature effect on cation sxchange is generally small, Various other workers (33) have found that the exchange reaction is accelerated somewhat by raising the temperature, Sen and Guha (34) found that on heating a kaolinite clay to 1,000°C, its cation exchange capacity showed no change until about 400°C. These observations suggest that the clay-water interaction which causes the permeability reduction at room

temperature **cannot** in itself explain the temperature dependence of permeability in the case of the water-saturated **cores.**

VI. CONCLUSIONS AND RECOMMENDATIONS

This experimental study has shown that permeabilitiea of consolidated sandstones are thermally sensitive under certain conditions. Several conclusions can be drawn from the results that have been presented. First of all, the temperature effect on permeability depends on the nature of the saturating fluid. In the case of water-saturated cores, permeability decreased with increasing temperature for all the samples studied. Over a temperature span of 70-325°F, permeability reductions of up to 65% were observed.

For oil-saturated samples, a slight increase in permeability with increasing temperature was observed in the low temperature range, followed by a decrease and an apparent stabilization. However, this thermal sensitivity barely exceeded the range of experinental error,

On the other hand, absolute Permeability to gas was found to be independent of temperature. Slip phenomena are affected by temperature and a linear relationship between the Klinkenberg slip factor and temperature was found and explained by analysis of theory. But the "extrapolated" or absolute permeability vas the same at all temperatures. Also, inertial ("turbulence") factors were determined and found to be independent of temperature.

One of the objectives of this work had been to simultaneously measure the effect of thermal stresses and mechanical stresses on permeability. It was found that regardless of the nature of

the saturating fluid, the level of confining pressure affecteci permeability in the same manner, i.e., permeability decreased with increasing confining pressure, For the thermally-sensitive water-saturated cores increasing the confining pressure had the additional effect of intensifying the temperature dependence.

In the light of the results obtained, it appears that the temperature effect was not caused by changes in the physical properties of the fluids, such as viscosity or density, because fluids with such a large viscosity and density contrast as oil and gas essentially yielded the same results; nor was the temperature effect caused by thermally induced mechanical stresses acting alone, as no significant permeability changes were found for oil or gas flow. Instead, the unique results obtained for water flow suggest that a combination of rock-fluid interaction, thermal stresses and mechanical stresses was responsible for the permeability reductions observed, the dominant factor being the surface effect.

Because the clay-water interaction, which is believed to have caused the permeability reduction, is due to the polarity of the water molecule, it is recommended that further work be conductei with other polar fluids, such as methanol or steam, in order to investigate the conclusions presented herein. The current interest in geothermal reservoirs certainly justifies additional research on water or steam flow at elevated temperatures, Also, since this work was limited to sandstones, it would be of great interest to conduct similar experiments on intergranular limestones. Additional study of the effect of firing temperature *and* the duration of the firing cycles when deactivating

the clay should be made. Study of the flow of oil in presence of a water saturation smaller than the irreducible water saturation could be a crucial test of the validity of the surface effects theory. Finally, the safety limits of the equipment used in this work could be extended to allow for higher values of confining pressures, possibly as high as 10,000 psi.

BIBLIOGRAPHY

1. Weinbrandt, RM: " The Effect of Temperature on **Relative** Permeability ", Ph.D. Dissertation, Stanford University (1972).

2. Casse, F.J.: "The Effect of Temperature on Absolute Permeability", M.S. Report, Stanford University (June, 1972).

3. Muskat, M.: The Flow of Homogeneous Fluids Through Porous Media , Mc Graw-Hill Book Company, Inc., 1937, p.71.and p.17.

4. Paaswell, R.E.: "Thermal Influence on Flow **from** a Compressible Porous Medium", Water Resources Research (1967), 3, No. 1,271.

5. Greenberg, D.B., Cresap, R.S., and Malone, **T.A.** : "Intrinsic Permeability of Hydrological Porous Mediums : Variation with Temperature", Water Resources Research (Aug., 1968), 4, No.4,791.

6. Afinogcnov, Y.A.: "How the Liquid Permeability of Rocks is Affected by Pressure and Temperature", SNIIGIMS (1969). No.6,34-42 (Translation from Consultants Bureau, 227 **West** 17th St., N.Y., N.Y. 10011).

7. Wilhelmi, B. and Somerton, W.H.: "Simultaneous Measurement of Pore and Elastic Properties of Rocks under **Triaxial Stress** Conditions", Soc.Pet.Eng.Jour.,(Sept.1967),240, 283.

8. [illegible], I. and [illegible]-isD.H.: "Reduction in Permeability with Overburden Pressure", Trans., AIME (1952) 195,329.

9. Mc Latchie, L.S., Hemstock, R.A., and Young, J.W.: "The Effect of Compressibility of Reservoir Rocks and Its Effect on Permeability", Trans., AIME (1958) 213,386.

10. Gray, H.E., Fatt, I., and Bergamini, G.: "The Effect of Stress on Permeability of Sandstone Cores", Soc. Pet. Eng. Jour. (June, 1963), 95.

11. Dobrynin, V.M.: "Effect of Overburden Pressure on Some Properties of Sandstones", Soc. Pet. Eng. Jour. (Dec., 1962) 2, No.4,360.

12. Zoback, M.D., and Byerlee, J.D. : "Permeability and Effective Stress", Bull. Am.Assoc. Pet. Geol., in press, 1974.

13. Wyble, D.O.: "Effect of Applied Pressure on the Conductivity, Porosity and Permeability of Sandstones", Trans. AIME (1958) 213, 431.

14. Sanyal, S.K., Marsden, S.S. and Ramey, H.J., Jr.: "The Effect of Temperature on Electrical Resistivity of Porous Media", SPWLA 13th Annual Logging Symposium, (May, 1972).

15. Sanyal, S.K., Ramey, H.J., Jr. and Marsden, S.S.: "The Effect of Temperature on Capillary Pressure Properties of Rocks", SPWLA 14th Annual Logging Symposium, (May, 1973).

16. Okandan, E.: "The Effect of Temperature and Fluid Composition on Oil-Water Capillary Pressure Curves of Limestone and Sandstones and Measurement of Contact Angles at Elevated Temperatures", Ph.D. Dissertation, Stanford U. (Nov., 1973).

17. Somerton, W.H., Mehta, M.M., and Dean, G.W.: "Thermal Alteration of Sandstones", J.Pet.Tech., (May,1965),234, I-589.

18. Edmondson, J.A.: "Effect of Temperature on Waterflooding", J. Gas. Pet. Tech. (1965) 4,236.

19. Davidson, L.B.: "The Effect of Temperature on the Permeability Ratio of Different Fluid Pairs in Two-Phase Systems", J. Pet. Tech. (Aug., 1969) 1037.

20. Poston, S.W., Ysrael, S.C., Hossain, A.K.M.S., Montgomery, R.F., [illegible], and Ramey, H.J., Jr.: "The Effect of Temperature on Irreducible Water Saturation and Relative Permeability of Unconsolidated Sands", Soc. Pet. Eng. J. (June, 1970) 171.

21. Lo, H.Y., and Mungan, N: "Effect of Temperature on Water–Oil Relative Permeabilities in Oil–Wet and Water–Wet Systems", paper SPE 4505 presented at the 48th Annual Fall Meeting, SPE of AIME, Las Vegas, Nev., Sept. 30 - Oct. 3, 1973.

22. Weinbrandt, R.M., Ramey, H.J., Jr. and Casse, F.J: "The Effect of Temperature on Relative and Absolute Permeability of Sandstones", 47th Annual Meeting of SPE of AIME, San Antonio, Texas (Oct., 1972).

23. Klinkenberg, L.J.: "The Permeability of Porous Media to Liquids and Gases", Drill, and Prod. Prac,, API (1941) 200.

24. Hirschfelder, J.O., Curtiss, C.F., and Bird, R.B. : Molecular Theory of Gases and Liquids , John Wiley & Sons, Inc., New York, London,

25. Forchheirner,' P. : "Hydraulik" Leipzig and Berlin, Chapter 15, Sections 116-118, Druck und Verlag von B.G. Teubner, 1914

26. Cornell, D. and Katz, D.L.: "Flow of Gases Through Consolidated Porous Media", Ind. Eng. Chem,, 1953, 45,2145.

27. Kolada, L.J.: "Steady Linear Gas Flow Through Porous Media" , Master's thesis, Department of Chemical and Petroleum Engineering, University of Alberta, 1967.

28. Dranchuk, P.M., and Kolada, L.J. : "Interpretation of Steady Linear Visco–Inertial Gas Flow Data", Jour.Can.Pet.Tech.,1968, 2, No.1,p 2n.

29. Somerton,W.H.,El-Shaarani, A.H., and Mobarak, S.M.: "High Temperature Behavior of Rocks Associated with Geothermal Type Reservoirs ", paper presented at the 44th Annual California Regional Meeting of the SPE of AIME, San Francisco, April 1974.

Grim,R.E. : "Applied Clay Mineralogy", McGraw-Hill Book Company,Inc, 1962.

31. Grim,R.E. : "Clay Mineralogy", McGraw-Hill Book Company, Inc., 1968.

32. Kelley, W.P.:"Cation Exchange in Soils", Rheinhold, New-York, 1948.

33. Kelley, W.P. ,and Brow, S.M. :"Replaceable Bases in Soils",Cal. Univ. Agr. Expt. Sta. Tech. Paper 15 (1924).

34. Sen, S.and Guha, S.K.:"The Effect of Heat on the Base Exchange Capacity of a Kaolinite Clay and its Structural Implications", Proc. Interm. Clay Conf., Stockholm,1963,1:215-229.

35. Perry,J.H.:Chemical Engineer's Handbook,McGraw-Hill Book Company, Inc., 1969, p23-10.

36. Arihara,N.:"A Study of Non-isothermal Single and Two-Phase Flow Through Consolidated Sandstones", Ph.D. dissertation, Nov.1974, Stanford University.

37. A.S.M.E. Steam Tables, 1967.

38. API RP 27:"Recommended Practice for Determining Permeability of Porous Media", Am.Pet.Inst.,(Aug.,1956).

39. Jones, S.C.:"A Rapid Accurate Unsteaay-State Klinkenberg Permeameter",Soc.Pet.Eng.Jour.,(Oct.,1972),12,No.4, 483.

40. KatzD.L.;and Coats,K.H.:Underground Storage of Fluids,Ulrich's Books, Inc., Ann Arbor, Michigan, 1968.

APPENDIX A

LIST OF TABULATED DATA

This Appendix contains all of the pertinent data that were obtained during the course of our experimental work. A separate table is presented for ehch one of the various core samples that were used in this study, These data either duplicate or complement the information given in Figs. 1 through 26,

Table 1 . Viscosity of Chevron White Oil No. 15 versus Temperature

T, °F	(1) α_T^*	(2) Δp (psi)	(3) q (cc/sec)	(1) x (2) / (3) μ (cp)	(4) Re**
73	0.05194 (calibration)	74.7	0.02456	158	0.20
76	0.05194	94.5	0.03769	130	0.38
99.5	0.05198	53.1	0.04312	64.0	0.87
150	0.05205	38.8	0.10592	19.1	7.05
200	0.05212	4.6	0.02924	8.2	4.45
250	0.05219	2.75	0.03259	4.4	9.02
300	0.05225	2.90	0.05574	2.72	24.54

* $\alpha_T = 0.05194\left[1+2.67\times10^{-5}(T-73)\right]$

** $Re = 50.124 \frac{q(cc/sec)\ \rho(g/cc)}{D(in)\ \mu(cp)}$

TABLE2 . INVESTIGATION OF HYSTERESIS - BOISE CORE #2

(Net confining pressure = 3700 psi)

Cycle number	T, °F	k, md	%perm.red. due to heating	%hysteresis at room cond.	Overall % hysteresis
-	71	2063	-	-	-
-	300	1340	35%	-	-
1	71	1651	-	20%	20%
	292	1253	24%	-	-
2	73	1551	-	6%	24.8%
	308	1060	32%	-	-
3	77	1481	-	4.5%	28.2%
	302	985	33.5%	-	-
4	74	1455	-	1.8%	29.5%
	305	1000	31%	-	-
5	74	1414	-	2.8%	31.5%

Table 3. Density of Chevron White Mineral Oil No.15 versus Temperature

Temperature, °F	Oil Volume, cc	Total Weight (flask+oil), g	Oil Weight*, g	
71	25.00	38.2124	21.5794	0.8631
100	25.02	37.9926	21.3596	0.8537
120	25.03	37.8396	21.2066	0.8470
150	25.04	37.6039	20.9710	0.8375
176	25.05	37.4014	≤0.7 84	0.8290

* Dry flask weight = 16.6330 g

Table 4. Viscosities of Nitrogen and Helium versus Temperature

Temperature, ^{o}F	Nitrogen Viscosity,* cp	Helium Viscosity,** cp
50	0.01713	0.01893
70	0.01764	0.01949
100	0.01839	0.02030
150	0.01959	0.02161
200	0.02074	0.02287
250	0.02185	0.02408
300	0.02291	0.02 2[illegible]
350	0.02394	0.026[illegible]

* $\mu_{N_2} = \frac{13.85\ 10^{-4}\ T^{1.5}}{102 + T}$

** $\mu_{He} = \frac{15.13\ 10^{-4}\ T^{1.5}}{97.6 + T}$

where T = temperature, ^{o}K

Table 5. Core Properties

Core No.	Length, cm	Diameter, cm	Area, cm^2	Porosity, %
Boise No.2	4.641	2.499	4.905	28.0
Boise No.3	5.039	2.499	4.905	28.1
Boise No.6	4.712	2.510	4.948	28.3
Boise No.7	5.273	2.527	5.016	28.2
Boise No.7F	4.458	2.527	5.016	28.2
Berea No.12	5.585	2.502	4.917	19.3
Berea No.14	5.491	2.530	5.027	18.8
Berea No.16	4.796	2.477	4.819	18.8
Berea No.17	5.189	2.535	5.047	18.5
Pandora No.29	5.502	2.451	4.718	22.1

Table6 . Experimental Data for Noise # 7, waterflow

$L = 5.273\ cm_2$
$A = 5.016\ cm^2$

Run No.	T_{room} (^oF)	T_{core} (^oF)	Δp (psi.)	W (g /sec)	ρ (g/cc)	p_c (psig)	μ (cp)	$k = \frac{14.7}{\Delta p} 10^3 \frac{L}{A} \mu \frac{W}{\rho}$ (mD)
7-2-1-1 & 7-2-1-2	75	75	4.5	.4295	1.000	2,000	.900	1,330
7-2-2-1 & 7-2-2-2	75	95	4.0	.4295	0.996	2,000	.715	1,189
7-2-3-1 & 7-2-3-2	75	125	3.55	.4295	0.990	2,000	.530	993
7-2-4-1 & 7-2-4-2	75	148	3.25	.4295	0.983	2,000	.436	892
7-2-5-1 & 7-2-5-2	75	175	3.0	.4295	0.975	2,000	.351	783
7-2-6-1 & 7-2-6-2	75	240	2.55	.4295	0.949	2,000	.240	626
7-2-7-1 & 7-2-7-2	75	315	2.25	.4295	0.910	2,000	.172	509

Table 7 . Experimental Data for Berea #12, water flow

$L = 5.585\ cm_2$
$A = 4.913\ cm^2$

Run No.	T_{room} (^oF)	T_{core} (^oF)	Δp (psi)	W (g/sec)	ρ (g/cc)	p_c (psig)	μ (cp)	$k = \frac{14.7}{\Delta p} 10^3 \frac{L}{A} \mu \frac{W}{\rho}$ (mD)
12-2-1-1 & 12-2-1-2	78	78	59.0	.4295	1.000	2,000	.872	106
12-2-2-1 & 12-2-2-2	78	139	37.5	.4295	0.985	2,000	.466	90
12-2-3-1 & 12-2-3-2	78	175	32.0	.4295	0.975	2,000	.353	81.2
12-2-4-1 & 12-2-4-2	78	235	28.0	.4295	0.951	2,000	.245	66.1
12-2-5-1 & 12-2-5-2	78	300	23.0	.4295	0.919	2,000	.1825	61.9

Table 8. Experimental Data for Berea #16, water flow

$L = 5.45$ cm
$A = 5.003$ cm^2

Run No.	T_{room} (°F)	T_{core} (°F)	Δp (psi)	W (g/sec)	ρ g/cc	p_c (psig)	μ (cp)	$k = \frac{14.7}{\Delta p} 10^3 \frac{L}{A} \mu \frac{W}{\rho}$ (mD)
16-2-1-1 &16-2-1-2	80	80	51.0	.4295	0.9	2,000	.845	113.9
16-2-2-1	80	170	26.5	.4295	0.975	2,000	.365	94.7
16-2-2-2 &16-2-2-3	80	170	27.0	.4295	0.975	2,000	.365	93.0
16-2-3-1	80	204	23.0	.4295	0.965	2,000	.292	87.3
16-2-3-2 &16-2-3-3	80	204	24.0	.4295	0.965	2,000	.292	83.7
16-2-4-1 &16-2-4-2	80	252	21.5	.4295	0.943	2,000	.227	72.6
16-2-5-1 &16-2-5-2	80	300	18.0	.4295	0.919	2,000	.182	69.5
16-2-6-1 &16-2-6-2	80	270	20.5	.4295	0.935	2,000	.207	69.4
16-2-7-1 &16-2-7-2	80	230	22.5	.4295	0.954	2,000	.251	76.7
16-2-8-1 &16-2-8-2	80	200	25.0	.4295	0.966	2,000	.300	82.5
16-2-9-1 &16-2-9-2	80	150	32.0	.4295	0.982	2,000	.425	91.3

Table 9. Experimental Data for Berea No.17, water flow

L = 5.19 cm_2
A = 5.05 cm^2

Run No.	T_{room} (°F)	T_{core} (°F)	Δp (psi)	W (g/sec)	ρ (g/cc)	p_c (psig)	μ (cp)	$k = \frac{14.7}{\Delta p} \times 10^3 \times \frac{L}{A} \times \mu \times \frac{W}{\rho}$ (mD)
17-04-1-1	74	74	36.0	0.267	1.000	450	.915	102.4
17-04-1-2	74	74	29.0	0.218	1.000	450	.915	104.0
17-04-2-1	74	200	11.6	0.247	0.966	450	.300	100.1
17-04-2-2	74	200	13.4	0.282	0.966	450	.300	99.1
17-04-3-1	74	292	7.2	0.234	0.923	450	188	100.0
17-04-3-2	74	292	7.5	0.235	0.923	450	.188	97.5
17-1-1	70	70	45.0	0.311	1.001	1,000	.960	100.2
17-1-2-1	71.5	141	20.7	0.297	0.985	1,000	.455	100.0
17-1-2-2	71.5	145	18.5	0.267	0.984	1,000	.441	98.0
17-1-3	71.5	198	14.4	0.284	0.906	1,000	.304	95.5
17-1-4-1	71.5	298	10.4	0.294	0.920	1,000	.185	85.7
17-1-4-2	71.5	298	10.6	0.307	0.920	1,000	185	87.0

Table 9. Experimental Data for Berea No.17, water flow, continued.

L = 5.19 cm
A = 5.05 cm^2

Run No.	T_{room} (°F)	T_{core} (°F)	Δp (psi)	W (g/sec)	ρ (g/cc)	p_c (psig)	μ (cp)	$k = \frac{14.7}{\Delta p} \times 10^3 \times \frac{L}{A} \times \mu \times \frac{W}{\rho}$ (mD)
17-2-1	70	70	44.0	0.298	1.001	2,000	.960	98.1
17-2-2-1	70	200	15.3	0.294	0.966	2,000	.300	90.5
17-2-2-2	70	200	12.7	0.248	0.966	2,000	.300	81.5
17-2-3	70	294	11.6	0.323	0.922	2,000	.186	80.8
17-3-1	74	74	37.5	0.262	0.993	3,000	.915	96.6
17-3-2	74	145	20.3	0.278	0.984	3,000	.441	93.0
17-3-3	74	200	13.9	0.262	0.966	3,000	.300	88.5
17-3-4-1	74	294	11.2	0.270	0.922	3,000	.186	73.8
17-3-4-2	74	294	12.0	0.294	0.922	3,000	.186	74.9
17-4-1	74	74	38.6	0.264	0.999	4,000	.915	94.5
17-4-2	74	145	20.7	0.276	0.984	4,000	.441	90.1
17-4-3	74	206	15.7	0.293	0.963	4,000	.290	85.4
17-4-4	74	294	13.0	0.294	0.922	4,000	.186	69.0

Table 10. Experimental Data for Boise No.2, water flow

$L = 4.64\ cm_2$
$A = 4.91\ cm^2$

Run No.	T_{room} (°F)	T_{core} (°F)	Δp (psi)	W (g/sec)	ρ (g/cc)	p_c (psig)	μ (cp)	$k = \frac{14.7}{\Delta p} \times 10^3 \times \frac{L}{A} \times \mu \times \frac{W}{\rho}$ (mD)
2-1-1-1	73	73	1.33	0.247	1.000	1,000	.925	2,388
2-1-1-2	73	76	1.46	0.281	1.000	1,000	.890	2,381
2-1-1-3	71	71	1.64	0.285	1.001	1,000	.950	2,295
2-1-2	73	149	0.76	0.274	0.983	1,000	.431	2,200
2-1-3	73	207	0.60	0.314	0.963	1,000	.288	2,178
2-4-1	71	71	1.49	0.233	1.001	4,000	.950	2,062
2-4-2	71	150	.96	0.292	0.982	4,000	.425	1,833
2-4-3	71	208	.67	0.271	0.962	4,000	.286	1,670
2-4-4	71	300	.78	0.284	0.919	4,000	.182	1,325
2-4-5	71.5	71.5	2.44	0.306	1.001	4,000	.945	1,647

Table11. Experimental Data for Boise No.7F, water flow, after firing to 760°C.

L = 4.46 cm_2
A = 5.02 cm^2

Run No.	T_{room} (°F)	T_{core} (°F)	Δp (psi)	W (g/sec)	ρ (g/cc)	p_c (psig)	μ (cp)	$k = \frac{14.7}{\Delta p} \times 10^3 \times \frac{L}{A} \times \mu \times \frac{W}{\rho}$ (mD)
7F-1-1	70	70	2.00	0.301	1.001	1,000	0.960	1,889
7F-1-2	74							
7F-1-3	74	203	0.63	0.289	0.965	1,000	0.295	1,837
7F-2-1	69	69	1.90	0.278	1,001	2,000	0.970	1,852
7F-2-2	74	144	0.92	0.283	0.985	2,000	0.445	1,817
7F-2-3	74	203	0.65	0.293	0.965	2,000	0.295	1,805
7F-3-1-1	70	70	1.96	0.283	1.001	3,000	0.960	1,813
7F-3-1-2	70	70	2.10	0.306	1.001	3,000	0.960	1,826
7F-3-2	74	145	0.93	0.284	0.984	3,000	0.442	1,788
7F-3-3	74	203	0.67	0.296	0.965	3,000	0.295	1,767
7F-4-1	70	70	1.98	0.282	1.001	4,000	0.960	1,784
7F-4-2	74	145	0.96	0.286	0.984	4,000	0.442	1,762
7F-4-3	70	205	0.66	0.284	0.964	4,000	0.292	1.705

Table 12. Viscous Flow Data for Bandera Core No.29, Nitrogen Flow.

L = 5.50 cm , A = 4.72 cm^2 , Confining Pressure = 2,000 psi

Run No.	p_1, psia	Δp, psi	p_m, psia	$14.7/p_m$, atm^{-1}	q_{room}, cc/sec	T_{room}, ^oK	T_{core}, ^oK	μ, cp	$k = \frac{L}{A} \cdot \mu \cdot \frac{14,700}{\Delta p \; p_m} \cdot q_{room} \cdot p_{room} \cdot \frac{T_{core}}{T_{room}}$
29-2-1-1	24.9	9.9	19.95	0.737	1.722	289.2	289.2	0.0174	38.2
29-2-1-2	30.2	15.2	22.6	0.650	2.964	289.2	289.2	0.0174	37.8
29-2-1-3	38.2	14.5	30.95	0.475	3.780	289.2	289.2	0.0174	36.9
29-2-1-4	56.7	13.3	50.05	0.294	5.47	289.2	289.2	0.0174	36.0
29-2-1-5	79.8	8.0	75.8	0.194	4.913	289.2	289.2	0.0174	35.5
29-2-2-1	23.5	6.1	20.45	0.719	1.145	290.0	371.4	0.0209	40.2
29-2-2-2	35.5	9.8	30.6	80	2.615	290.0	3 4	0.0209	8.2
29-2-2-3	55.9	12.9	49.45	97	5.329	290.0	3 4	0.0209	6.6
29-2-2-4	95.7	7.0	92.2	0.159	5.185	290.0	371.4	0.0209	35.2
29-2-3-1	22.2	7.1	18.65	0.788	1.275	290.0	410.3	0.0225	42.2
29-2-3-2	42 7	12.2	36.6	0.402	3.883	290.0	410.3	0.0225	38.1
29-2-3-3	46.2	8.5	41.95	0.350	3.052	290.0	410.3	0.0225	37.5
29-2-3-4	54.1	10.2	49.0	0.300	4.209	290.0	410.3	0.0225	36.9
29-2-4-1	30.0	14.6	22.68	0.648	3.124	290.0	426.4	0.0231	41.2
29-2-4-2	36.7	13.4	30.0	0.490	3.615	290.0	426.4	0.0231	39.4
29-2-4-3	44.6	14.2	37.5	0.392	4.667	290.0	426.4	0.0231	38.4

Table 12. Viscous Flow Data for Bandera Core No.29, Nitrogen Flow.(continued)

L = 5.50 cm . A = 4.72 cm^2 . Confining Pressure = 2,000 psi

Run No.	p_1, psia	Δp, psi	p_m, psia	$14.7/p_m$, atm^{-1}	q_{room}, cc/sec	T_{room}, ^oK	T_{core}, ^oK	μ, cp	$k = \frac{L}{A} \times \mu \times \frac{14,700}{\Delta p\ p_m} \times q_{room} \times p_{room} \times \frac{T_{core}}{T_{room}}$
29-2-4-4	46.7	8.5	42.45	0.346	3.113	290.0	426.4	0.0231	37.8
29-2-4-5	59.1	11.4	53.43	0.275	5.186	290.0	426.4	0.0231	37.3
29-2-4-6	78.7	9.3	74.05	0.199	5.674	290.0	426.4	0.0231	36.1

Table 13. Viscous Flow Data for Berea Core No.12, Nitrogen Flow.

L = 5.59 cm , A = 4.92 cm^2 , Confining Pressure = 2,000 psi

Run No.	p_1, psia	Δp, psi	p_m, psia	$14.7/p_m$, atm^{-1}	q_{room}, cc/sec	T_{room}, ^oK	T_{core}, ^oK	μ, cp	$k = \frac{L}{A} \times \mu \times \frac{14,700}{\Delta p \; p_m} \times q_{room} \times p_{room} \times \frac{T_{core}}{T_{room}}$
12-2-1-1	24.2	8.2	20.1	0.731	5.841	289.2	289.2	0.0174	151.4
12-2-1-2	30.2	3.4	28.5	0.516	3.414	289.2	289.2	0.0174	150.5
12-2-1-3	51.4	2.7	50.05	0.294	4.622	289.2	289.2	0.0174	146.1
12-2-1-4	62.2	1.9	61.25	0.240	3.958	289.2	289.2	0.0174	145.3
12-2-1-5	76.3	1.55	75.53	0.195	3.946	289.2	289.2	0.0174	144.0
12-2-2-1	22.2	3.9	20.25	0.726	2.284	290.1	329.8	0.0192	155.0
12-2-2-2	32.3	4.4	30.1	0.488	3.732	290.1	329.8	0.0192	151.0
12-2-2-3	53.05	2.4	51.85	0.284	3.409	290.1	329.8	0.0192	146.8
12-2-2-4	66.9	2.5	65.63	0.224	4.458	290.1	329.8	0.0192	145.6
12-2-3-1	25.8	3.1	24.25	0.606	1.771	290.8	371.4	0.0209	154.4
12-2-3-2	33.5	7.3	29.85	0.492	5.081	290.8	371.4	0.0209	152.8
12-2-3-3	56.5	5.1	53.95	0.272	6.222	290.8	371.4	0.0209	148.2
12-2-3-4	56.6	2.7	55.25	0.266	3.351	290.8	371.4	0.0209	147.2
12-2-4-1	22.0	5.8	19.1	0.770	2.157	291.0	426.4	0.0231	161.8
12-2-4-2	26.7	3.8	24.83	0.592	1.758	291.0	426.2	0.0231	156.9
12-2-4-3	56.7	3.1	55.15	0.267	3.080	291.0	426.4	0.0231	149.7
12-2-4-4	79.1	2.9	77.65	0.189	3.994	291.0	426.4	0.0231	147.4

Table 14. Viscous Flow Data for Berea Core No.16, Nitrogen Flow.

L = 5.45 cm , A = 5.80 cm^2 , Confining Pressure = 600 psi

Run No.	p_1, psia	Δp, psi	p_m, psia	$14.7/p_m$, atm^{-1}	q_{room}, cc/sec	T_{room}, ^oK	T_{core}, ^oK	μ, cp	$k = \frac{L}{A} \mu \frac{14,700}{\Delta p\ p_m} q_{room} p_{room} \frac{T_{core}}{T_{room}}$
16-06-1-1	21.8	2.88	20.36	0.727	1.968	293.7	293.7	0.0176	140.1
16-06-1-2	27.9	4.74	25.53	0.580	4.016	293.7	293.7	0.0176	138.5
16-06-1-3	28.3	4.68	25.96	0.566	4.08	293.7	293.7	0.0176	139.1
16-06-1-4	28.0	1.68	27.16	0.545	1.538	293.7	293.7	0.0176	138.5
16-06-1-5	28.0	1.66	27.17	0.545	1.488	293.7	293.7	0.0176	137.6
6-06-1-6	42.5	2.16	41.42	0.357	2.930	293.7	293.7	0.0176	136.7
16-06-1-7	160.7	0.93	160.2	0.092	4.81	293.7	293.7	0.0176	133.5
16-06-2-1	21.8	2.87	20.35	0.726	1.58	292.0	338.1	0.0196	145.2
16-06-2-2	23.2	2.85	21.84	0.676	1.677	292.0	338.1	0.0196	145.0
16-06-2-3	44.0	1.78	23.09	0.640	1.107	292.0	338.1	0.0196	144.4
16-06-2-4	29.8	4.25	27.66	0.534	3.125	292.0	338.1	0.0196	142.5
16-06-2-5	30.0	1.64	29.26	0.505	1.27	292.0	338.1	0.0196	141.9
16-06-2-6	42.1	1.97	41.1	0.360	2.119	292.0	338.1	0.0196	140.2
16-06-2-7	104.8	0.78	104.4	0.142	2.062	292.0	338.1	0.0196	135.7
16-06-3-1	24.4	2.38	23.23	0.638	1.174	293.1	394.2	0.0218	147.9
16-06-3-2	29.3	5.0	26.82	0.553	2.80	293.1	394.2	0.0218	145.5

Table 14. Viscous Flow Data for Berea Core No.16, Nitrogen Flow.

L = 5.45 cm , A = 5.00 cm^2 , Confining Pressure = 600 psi

Run No.	p_1, psia	Δp, psi	p_m, psia	$14.7/p_m$, atm^{-1}	q_{room}, cc/sec	T_{room}, ^oK	T_{core}, ^oK	μ, cp	$k = \frac{L}{A} \times \mu \times \frac{14,700}{\Delta p \; p_m} \times q_{room} \times p_{room} \times \frac{T_{core}}{T_{room}}$
16-06-3-3	32.8	4.5	30.57	0.485	2.84	293.1	394.2	0.0218	140.8
16-06-3-4	41.4	2.25	40.3	0.368	1.845	293.1	394.2	0.0218	141.8
16-06-3-5	109.3	0.68	109.0	0.136	1.459	293.1	394.2	0.0218	137.2
16-06-4-1	23.9	1.88	22.9	0.648	0.776	293.1	436.4	0.0235	149.6
16-06-4-2	27.5	0.97	27.0	0.551	0.463	293.1	436.4	0.0235	146.9
16-06-4-3	34.8	5.2	32.2	0.460	2.985	293.1	436.4	0.0235	146.2
16-06-4-4	34.9	4.77	32.48	0.458	2.688	293.1	436.4	0.0235	144.1
16-06-4-5	34.9	1.4	34.16	0.435	0.825	293.1	436.4	0.0235	143.6
16-06-4-6	41.8	2.23	40.75	0.365	1.567	293.1	436.4	0.0235	143.2
16-06-4-7	71.5	1.04	70.95	0.209	1.229	293.2	436.4	0.0235	138.3
16-06-4-8	70.8	2.45	69.54	0.214	2.833	293.1	436.4	0.0235	138.1
16-06-4-9	106.0	0.86	105.5	0.141	1.502	293.1	436.4	0.0235	136.9

Table 15. Viscous Flow Data for Berea Core No.16, Helium Flow.

L = 5.45 cm , A = 5.00 cm^2 , Confining Pressure = 600 psi

Run No.	p_1, psia	Δp, psi	p_m, psia	$14.7/p_m$, atm^{-1}	q_{room}, cc/sec	T_{room}, ^oK	T_{core}, ^oK	μ, cp	$k = \frac{L}{A} \times \mu \times \frac{14,700}{\Delta p\ p_m} \times q_{room} \times p_{room} \times \frac{T_{core}}{T_{room}}$
16-06-5-1	21.5	4.05	19.43	0.764	2.646	292.0	292.0	0.0194	154.9
16-06-5-2	21.9	2.62	20.54	0.723	1.805	292.0	292.0	0.0194	154.5
16-06-5-3	26.9	3.19	25.26	0.588	2.618	292.0	292.0	0.0194	149.7
16-06-5-4	27.-	[redacted]	[redacted]	0.58[illegible]	2.732	292.0	292.0	0.0194	151.3
16-06-5-5	27.0	3.21	25.35	0.586	2.632	292.0	292.0	0.0194	149.0
16-06-5-6	39.2	3.93	37.19	0.399	4.545	292.0	292.0	0.0194	143.3
16-06-5-7	40.4	2.26	39.22	0.379	2.762	292.0	292.0	0.0194	143.6
16-06-5-8	65.0	29.0	50.45	0.294	44.2	292.0	292.0	0.0194	139.2
16-06-5-9	78.4	1.88	77.41	0.192	4.31	292.0	292.0	0.0194	136.4
16-06-5-10	78.7	1.24	78.03	0.190	2.874	292.0	292.0	0.0194	136.8
16-06-5-11	109.[illegible]	0.9	108.8	0.137	3.067	292.0	292.0	0.0194	136.7
16-06-5-12	108.[illegible]	0.9	108.1	0.137	3.086	292.0	292.0	0.0194	135.6

Table 16. Visco-inertial flow data for Berea core No.16, nitrogen flow.

L = 5.45 cm , A = 5.80 cm^2 , Confining Pressure = 600 psi

Run No.	p_1, psia	Δp, psi	p_m, psia	$14.7/p_m$, atm^{-1}	q_{room}, cc/sec	T_{room}, ^oK	T_{core}, ^oK	μ, cp	$k = \frac{L}{A} \times \mu \times \frac{14,700}{\Delta p \; p_m} \times q_{room} \times p_{room} \times \frac{T_{core}}{T_{room}}$
VI-1-1	175.7	20.8	165.3	0.089	79.0	293.7	293.7	0.0176	95.1
VI-1-2	109.3	31.0	93.8	0.158	70.0	293.7	293.7	0.0176	98.2
VI-1-3	176.2	15.5	168.5	0.087	63.5	293.7	293.7	0.0176	100.7
VI-1-4	83.2	17.3	74.57	0.199	35.1	293.7	293.7	0.0176	113.7
VI-1-5	83.3	14.4	76.1	0.195	30.3	293.7	293.7	0.0176	115.5
VI-1-6	61.0	22.5	49.7	0.298	31.4	293.7	293.7	0.0176	116.7
VI-1-7	55.8	20.9	45.4	0.327	27.0	293.7	293.7	0.0176	118.8
VI-1-8	218.7	4.3	216.4	0.068	26.0	293.7	293.7	0.0176	115.7
VI-1-9	100.0	4.65	97.7	0.152	13.6	293.7	293.7	0.0176	124.0
VI-1-10	73.2	2.41	72.0	0.205	5.435	293.7	293.7	0.0176	129.6
VI-1-11	110.7	1.16	110.1	0.133	4.00	293.7	293.7	0.0176	129.6
VI-1-12	152.8	43.6	131.0	0.113	98.0	292.0	338.1	0.0196	92.0
VI-1-13	125.8	37.9	106.8	0.138	76	292.0	338.1	0.0196	100.6
VI-1-14	125.8	13.6	119.0	0.124	35	292.0	338.1	0.0196	115.9
VI-1-15	213.8	4.84	211.4	0.070	23	292.0	338.1	0.0196	120.5
VI-1-16	225.3	30.0	210.3	0.070	105.5	292.0	338.1	0.0196	89.6

Table 16. Visco-inertial flow data for Berea core No.16, nitrogen flow. (continued)

L = 5.45 cm , A = 5.80 cm^2 , Confining Pressure = 600 psi

Run No.	p_1, psia	Δp, psi	p_m, psia	$14.7/p_m$, atm^{-1}	q_{room}, cc/sec	T_{room}, ^oK	T_{core}, ^oK	μ, cp	$k = \frac{L}{A} \times \mu \times \frac{14,700}{\Delta p\ p_m} \times q_{room} \times p_{room} \times \frac{T_{core}}{T_{room}}$
VI-1-17	219.8	42.3	198.7	0.075	111.5	293.1	394.2	0.0218	92.4
VI-1-18	258.8	53.2	232.2	0.064	146.5	293.1	394.2	0.0218	82.6
VI-1-19	163.8	21.7	153.0	0.097	53.0	293.1	394.2	0.0218	118.6
VI-1-20	80.0	20.9	69.6	0.213	26.0	293.1	394.2	0.0218	124.6
VI-1-21	230.3	56.9	201.9	0.073	125.5	293.1	436.4	0.0235	90.7
VI-1-22	170.3	52.3	141.6	0.105	96.5	293.1	436.4	0.0235	98.4
VI-1-23	170.8	36.5	152.6	0.097	72.0	293.1	436.4	0.0235	107.2
VI-1-24	172.3	19.0	162.8	0.091	43.5	293.1	436.4	0.0235	116.7
VI-1-25	217.4	4.3	215.3	0.069	14.3	293.1	436.4	0.0235	128.2

Table 17 Experimental Data for Berwa #14, oil flow

L = 5.49 cm
A = 5.03 cm^2

Run No.	T_{room} (°F)	T_{core} (°F)	Δp (psi)	W (g/sec)	ρ (g/cc)	p_c (psig)	μ (cp)	$k = \frac{14.7}{\Delta p} \times 10^3 \times \frac{L}{A} \times \mu \times \frac{W}{\rho}$ (mD)
14-2-1-1	70	70	315.5	0.0125	0.864	2,000	190	137.0
14-2-1-2	71	71	314.5	0.0125	0.863	2,000	185	133.0
14-2-1-3	72	72	272	0.0114	0.863	2,000	167	130.0
14-2-1-4	75	75	341	0.0167	0.862	2,000	139	127.0
14-2-2-1	75	150	210.5	0.0752	0.838	2,000	19.1	130.0
14-2-2-2	75	150.5	211	0.0764	0.837	2,000	19	132.0
14-2-3-1	71	225	124.5	0.1468	0.813	2,000	5.9	137.0
14-2-3-2	71	225.5	94.5	0.1112	0.813	2,000	5.9	137.0
14-2-4-1	72	298.5	40.5	0.0920	0.789	2,000	2.8	129.0
14-2-4-2	72	298.5	42	0.0912	0.789	2,000	2.8	124.0

Table 18. Experimental Data for Boise No. 6, oil flow

$L = 4.71$ cm
$A = 4.95$ cm^2

Run No.	T_{room} (°F)	T_{core} (°F)	Δp (psi)	W (g/sec)	ρ (g/cc)	p_c (psig)	μ (cp)	$k = \frac{14.7}{\Delta p} \times 10^3 \times \frac{L}{A} \times \mu \times \frac{W}{\rho}$ (mD)
6-2-1-1	73.5	73.5	19.6	0.0188	0.862	2,000	153	2,383
6-2-1-2	80.5	80.5	11.8	0.0151	0.860	2,000	120	2,499
6-2-2-1	74	146	8.0	0.0587	0.839	2,000	20.6	2,521
6-2-2-2	74	146	7.9	0.0587	0.839	2,000	20.6	2,562
6-2-3-1	74	225	10.2	0.2553	0.813	2,000	5.9	2,540
6-2-3-2	74	225	10.4	0.2571	0.813	2,000	5.9	2,513
6-2-4-1	74	298.5	4.75	0.2535	0.789	2,000	2.65	2,510
6-2-4-2	74	298.5	5.0	0.2623	0.789	2,000	2.65	

Table 19. Experimental Data for Boise No.3, oil flow

$L = 5.04$ cm
$A = 4.91$ cm^2

Run No.	T_{room} (°F)	T_{core} (°F)	Δp (psi)	W (g/sec)	ρ (g/cc)	p_c (psig)	μ (cp)	$k = \frac{14.7}{\Delta p} \times 10^3 \times \frac{L}{A} \times \mu \times \frac{W}{\rho}$ (mD)
3-05-1-1	75	75	23.3	0.0183	0.862	500	139	1,908
3-05-1-2	80	80	35.2	0.0335	0.860	500	115	1,914
3-05-1-3	75	75	88.9	0.0717	0.862	500	139	1,959
3-05-2-1	75	149.5	9.0	0.0545	0.836	500	19.3	2,111
3-05-2-2	75	148.5	8.9	0.0534	0.8365	500	19.5	2,143
3-05-3	75	222	6.3	0.1197	0.814	500	6.15	2,179
3-05-4-1	75	299	4.	0.1825	0.789	500	2.8	2,214
3-05-4-2	75	299	4.5	0.1852	0.789	500	2.8	2,222
3-2-1	75	75	20.75	0.0156	0.863	2,000	155	1,835
3-2-2-1	75	150	8.65	0.0488	0.836	2,000	19.1	1,944
3-2-2-2	75	148	11.325	.04	0.837	2,000	1	1,995
3-2-3-1	75	223.5	6.34	0.111	0.810	2,000		1,960

Table 19. Experimental Data for Boise No. 3, oil flow, continued.

$L = 5.04$ cm
$A = 4.91$ cm^2

Run No.	T_{room} (°F)	T_{core} (°F)	Δp (psi)	W (g/sec)	ρ (g/cc)	p_c (psig)	μ (cp)	$k = \frac{14.7}{\Delta p} \times 10^3 \times \frac{L}{A} \times \mu \times \frac{W}{\rho}$ (mD)
3-2-3-2	75	224	8.4	0.1486	0.810	2,000	6.0	1,978
3-2-4-1	75	300	4.0	0.1488	0.789	2,000	2.72	1,936
3-2-4-2	75	296.5	4.4	0.1610	0.790	2,000	2.82	1,972
3-2-4-3	75	296.5	4.58	0.1697	0.790	2,000	2.82	1,997
3-4-1-1	73.5	73.5	22.5	0.0141	0.862	4,000	155	1,704
3-4-4-2	71	71	23.03	0.0139	0.863	4,000	170	1,795
3-4-2-1	71	148	15.4	0.0778	0.838	4,000	20.0	1,819
3-4-2-2	71	147.5	16.35	0.0829	0.838	4,000	20.0	1,827
3-4-3-1	71	188.5	7.55	0.0759	0.825	4,000	10.0	1,840
3-4-3-2	71	189	7.52	0.0757	0.825	4,000	10.0	1,843
3-4-4-1	71	295	4.23	0.1409	0.790	4,000	2.85	1,814
3-4-4-2	71	297	2.68	0.0918	0.790	4,000	2.81	1,844

APPENDIX B

ANALYSIS OF GAS FLOW DATA

1. DARCY'S LAW FOR GAS FLOW

The integrated form of Darcy's law which describes horizontal linear gas flow, under steady state, isothermal conditions is :

$$q_{room} = \frac{k\ A\ T_{room}\ \Delta p\ p_m}{\mu\ \bar{z}\ T\ p_{room}\ L} \qquad (B-1)$$

where :

q_{room} = gas flow rate at room conditions, cc/sec

k = absolute permeability, darcies

A = cross sectional area of porous medium, cm2

L = length of porous medium, cm

T_{room} = room temperature, ^oK

T = flowing temperature, ^oK

p_{room} = room pressure, atm. abs.

Δp = pressure drop across porous medium, atm

p_m = mean pressure within porous medium, atm. abs.

μ = gas viscosity at T and p_m, cp

$\bar{z}$ = mean gas compressibility factor

The foregoing set of units is consistent and no conversion factor is necessary, However, in laboratory work, pressures are usually measured in psi and permeabilities in millidarcies. For these units, the righthand side of Eq. B-1 must be divided by 14,700.

2. KLINKENBERG EFFECT

Klinkenberg [23] observed in 1941 that porous media showed a greater permeability to gases than to liquids, and concluded that this phenomenon was due to gas slippage at the surface of the rock. He further showed, on the basis of both theory and experimentation that the apparent permeability observed with gases was linearly related to the reciprocal mean pressure. This can be expressed by the following relationship:

$$k_a = k \left(1 + \frac{b}{\bar{P}}\right) \qquad \text{(B-2)}$$

where k is the true liquid permeability (or apparent permeability extrapolated to an infinita mean pressure).

Klinkenberg's theoretical approach to the slip phenomenon was based on a simplified conceptual model which consisted of randomly oriented capillaries of same radius r . The "b" factor in Eq. B-2 is determined experimentally and has been termed the "Klinkenberg slip factor". In his theoretical analysis, Klinkenberg derived an equation similar to B-2 by showing that:

$$k_a = k \left(1 + \frac{4\, c\, \lambda}{r}\right) \qquad \text{(B-3)}$$

where $\bar{\lambda}$ is the mean free path of the gas molecules (or average distance traversed by a molecule between collisions) and c is a proportionality factor. Because $\bar{\lambda}$ is inversely proportional to the pressure, Eqns. B-2 and. B-3 are strictly identical. As a result of the foregoing observations, b ha6 been generally acknowledged to be a constant for a given gas and a given porous medium. However, a rigorous statistical approach to the kinetic theory of gases (24) shows that the mean free path is also directly proportional to temperature: $\bar{\lambda} = c' \frac{T}{p\sigma^2}$ where σ is the collision diameter of molecules, and c' is a proportionality factor.

Substituting this value for $\bar{\lambda}$, Eq. B-3 may be rewritten:

$$k_a = k \left(1 + b' \frac{T}{P}\right) \qquad (B-4)$$

where b' is a constant for a given gas and a given porous ne-dium, To our knowledge this temperature dependency of b has not been recognized previously. The Klinkenberg slip factor is the product of b' and the absolute temperature at which the gas is flowing.

3. VISCO-INERTIAL FLOW

Darcy's law and the preceding equations are valid when conditions of viscous flow prevail. At high flow rates, Darcy's law I a not valid, and flow has been shown to be des-cribed by a quadratic equation. Such an equation was proposed

by Forchheiner (25) and modified by Corncll and Katz (26) as follows:

$$-\frac{dp}{dL} = \alpha \mu q + \beta \rho q^2 \qquad \text{(B-5)}$$

For the particular case of horizontal linear gas flow, in the absence of **slippage,** the integrated. form of (B-5) is:

$$\frac{p_m \Delta p}{\mu \bar{z} \frac{L}{A} \frac{T}{T_{room}} p_{room} q_{room}} = \alpha + \beta \frac{\rho q}{A \mu} \qquad \text{(B-6)}$$

For viscous flow, the quadratic term of B-5 is small enough to be neglected, and B-6 becomes identical to Eq.B-1. Therefore, we see that α has to be the reciprocal of permeability, i.e.: $\alpha = \frac{1}{k}$

The assumption of no gas slippage is Generally not critical because the high flow rates that arc responsible for turbulent flow have often been initiated by a pressure incrcasc, so that the mean pressure is relatively high. In such a case, gas slippage, as expressed by B-4, becomes negligible and α is actually the reciprocal of permeability. In many practical cases, turbulent flow a N gas slippage occur simultaneously. Tnis is especially true for systems where no backpressure is applied, and where the pressure drop is high enough to create large flow rates, while the mean pressure is kept at a relatively small valuc. The most rigorous way to account for *gas* slippage and turbulent flow simultaneously would be to replace α by

$\frac{1}{k\,(1+\frac{b}{P})}$ in B-5 and carry out the integration of the differential equation so obtained. This would result in a much more complex equation than Eq.B-6 which would have to be solved for β , b and k simultaneously, A numerical procedure would have to be developed and used on a digital computer. This kind of work was done by Kolada [27] in 1967. However, Dranchuk and Kolada [28] showed that gas slippage can be satisfactorily handled by replacing α by $\frac{1}{k(1+\frac{b}{p_m})}$ in Eq. B-6,

After multiplying through by $(1+\frac{b}{p_m})$ we obtain:

$$\frac{p_m \; p\,(1+\frac{b}{p_m})}{\mu\,\bar{z}\,\frac{L}{A}\,\frac{T}{T_{room}}\,p_{room}\,q_{room}} = \frac{1}{k} + \frac{q}{A\mu}\,(1+\frac{b}{p_m}) \qquad (B\text{-}7)$$

Eq. B-7 is of the form: $Y = \frac{1}{k} + \beta X$

Therefore, a graph of $Y = \frac{p_m\,p\,(1+b/p_m)}{\mu\,\bar{z}\,\frac{L}{A}\,\frac{T}{T_{room}}\,p_{room}\,q_{room}}$ vs. $X = \frac{q}{Au}\,(1+b/p_m)$

should yield a straight line of slope β and. intercept $\frac{1}{k}$, provided that the value of b is known.

In order to avoid a trial-and-error procedure, an appropriate reduction of the data can be made, so that b can be calculated as the slope of a conventional Klinkenberg straight line. This will also yield a value of k and, if the proper reduction has been made, this value of k will coincide with the one calculated from the visco-inertial flow data.

APPENDIX C

MINERALOGICAL COMPOSITION OF SANDSTONES

Boise, Berea and Bandera sandstones have been widely used in laboratory work and, as a result, they are well documented. The following Table and description were taken from ref.29. Even though the mineralogical composition of a given sandstone may vary from one sample to another, the figures presented hereafter do provide reasonable estimates of the composition of these rocks and particularly of their clay content.

MINERAL	BOISE	BEREA	BANDERA
Quartz	.387	,678	.555
Feldspar	.199	.015	.019
Plagioclase	,183	,012	.019
K-spar	,016	.003	
Calcite		.094	,166
Kaolinite and Matrix	.348	.190	.212
Muscovite Fe/Mg Minerals and Opaques	.016	.014	.020

APPENDIX C (continued)

BANDERA : Very fine grained, well compacted, quartzose sandstone. A large fraction of the primary feldspar grains have been partially to totally altered to kaolinite and in some cases the alteration continues on to muscovite. The matrix clay appears to be altered to kaolinite. Secondary calcite is variable in amount and may range from 10–25 percent in the thin-sections. The quartz grains are sub-angular to sub-rounded, The average permeability of the samples used in this study was 35md, and the average porosity about 22%.

BEREA : Fine grained, well compacted, quartzose sandstone. Partial and sometimes total replacement of unstable feldspar grains and matrix clay by kaolinite and where alteration sequence has continued, by muscovite. Secondary calcite is present and is variable in relative amount. Quartz grains are sub-angular to sub-rounded. The average permeability of the samples used in this study was 100md, and the average porosity about 19%.

BOISE : Medium-fine grained, well compacted, feldspar-quartzose sandstone. A large mount of the feldspar and matrix clay is altered to kaolinite, and, where alteration sequence has continued, to muscovite. Calcite is not present. Quartz grains are angular to sub-

angular. This sandstone is immature both texturally and mineralogically. The average permeability of the samples used in this study was 2,000md, and the average porosity about 28%.

APPENDIX D

LIST OF MANUFACTURERS AND SUPPLIERS

The following is a list of the various pieces of equipment or supplies that were selected for this work, together with the corresponding names of manufacturers and/or suppliers from whom they were acquired.

Chevron White Mineral Oil No.15 - Van Waters & Rogers, Inc., San Francisco.

Pressure Transducers - Dynasciences Corp., Model KP 15, c/o Gaao Instrument Sales, 655 Castro Street, Suite 2, Mountain View, Cal. 94040 (961-2222).

Barnett Industrial Dead Weight Tester - c/o Gado Instrument Sales, 655 Castro Street, Suite 2, Mountain View, Cal. 94040 (961-2222).

Pressure Indicator - Pace Model CD 25, c/o Gad Instrument Sales, 655 Castro Street, Suite 2, Mountain View, Cal. 94040 (961-2222).

Pressure Regulator - Volumetrics, Model VRC-400, 1025 Arbor Vitae Street, Inglewood, Cal. 90301 (213) 641-3747, or c/o Gaco Instrument Sales, 655 Castro Street, Suite 2, Mountain View, Cal. 94040 (961-2222).

High Pressure Regulator - Model 4-580, Matheson Gas Products, Newark, Cal., (793-2559).

Recording Potentiometer (for Pressure) - Heath Kit, Model EU-208, 2001 Middlefield Road, Redwood City, Cal., (365-8155).

Variable Rate Oil Pump - Model PC, Whitey Tool & Die Company, 5679 Landregan Emvl., Oakland, Cal, (653-5100) loan from USBM.

Hydraulic Hand Pump - Enerpac, Model P-39, Paul Monroc Hydraulics, Inc., 1570 Gilbreth Roac, Burlingame, Cal. 94010 (697-2950).

Constant Rate Pump - Hand maae equivalent to Ruska 2200 series Uses Viton O ring with machined teflon back up ring,

Accumulators (Greerolator), Model No.20-30 TMR-S-½ WS, Hydraulic Controls, Inc,, 1330 6th Street, Emeryville, Cal. 94608 (658-8300).

Recording Potentiometer (for temperature) - Model Speeao Max W, Leeds & Morthrup, 1095 Market Street, San Francisco (349-6656).

Thermocouples, Iron-Constantan, Conax, c/o Instrument Laboratory 644 Emerson Street, Palo Alto, Cal. 94303 (328-1040).

Temperature Controller - API Model 228 with 4010 Power Pack, API Instruments, 2339 Charleston Road, Mountain View, Cal. 94040 (964-0512).

Laboratory Flowrator Kit - Model No.10A3565ALKZ, Fisher & Porter Company, 1341 North Main Street, Walnut Creek, Cal. 94596 (933-8850).

Core Sleeve - Viton A tubing, West American Rubber Co., 750 North Main Street, Orange, Cal. 92668 (714-532 3355).

O Rings - Viton A with teflon backup rings, ABSCOA Industries, 880 Hurlingame Ave., Redwood City, Cal. (369-4897) or 1071 West Arbor Vitae Street, Inglewood, Cal. (213-7764561).

Tubing - Tubesales, 500 Sansome Street, San Francisco, Cal. (EN 1-1919).

Fittings & Valves - Van Dyke & Fitting Co., 5525 Marshal Street, Oakland, Cal. (658-1700).

Gas Analyzer - Gas Master, Laboratory Moael, GOW-MAC Instrument Co., 100 Kings Roac, Maciison, N.J. 07940 (201) 377-3450 or Applied Instrument Co., 199 1st Street, Los Altos (941-5928).